UC Berkeley
SEMM Reports Series

Title

Review of the behavior of a code compliant structural design under realistic case scenarios of seismic hazard demand

Permalink

https://escholarship.org/uc/item/98w7533r

Authors

Arteta, Carlos
Moehle, Jack

Publication Date

2014-04-01

eScholarship.org Powered by the California Digital Library
University of California

UCB/SEMM-2014/04

STRUCTURAL ENGINEERING

MECHANICS AND MATERIALS

REVIEW OF THE BEHAVIOR OF A CODE COMPLIANT STRUCTURAL DESIGN UNDER REALISTIC CASE SCENARIOS OF SEISMIC HAZARD DEMAND

by

Carlos A. Arteta

Jack P. Moehle

A paper submitted in partial satisfaction of the requirements for the degree of Master of Engineering in Civil and Environmental Engineering in the Graduate Division of the University of California at Berkeley.

DEPARTMENT OF CIVIL ENGINEERING

UNIVERSITY OF CALIFORNIA

BERKELEY, CALIFORNIA

In memory of my father. The person I have loved the most. He would have enjoyed reading and discussing this paper with me.

ACKNOWLEDGMENTS

This work, like all of the academic studies I have undertaken at the University of California, Berkeley, has been supported by the Fulbright Program, through the Faculty Development Program administered by LASPAU and by Universidad del Norte, Colombia. My most sincere gratitude to these institutions that made possible the enjoyment of this magnificent experience.

TABLE OF CONTENTS

1 **INTRODUCTION** 8

1.1 MOTIVATION 8

1.2 OBJECTIVES AND SCOPE 8

1.3 ORGANIZATION 9

2 **SEISMIC HAZARD ESTIMATION** 10

2.1 INTRODUCTION 10

2.2 SITE LOCALIZATION AND PARAMETERS TO ESTIMATE REALISTIC SEISMIC DEMAND 10

2.3 CODE BASED SEISMIC DESIGN CRITERIA 10

2.4 GROUND MOTION SELECTION PROCEDURE FOR NONLINEAR DYNAMIC ANALYSIS 11

2.5 RESPONSE SPECTRA COMPARISON 12

3 **STRUCTURAL MODEL** 13

3.1 INTRODUCTION 13

3.2 GEOMETRIC DESCRIPTION AND MATERIAL'S STRENGTH 13

3.2.1 Structures' Geometry 13

3.2.2 Selected Materials 14

3.3 ELASTIC ANALYSIS 15

3.4 DESIGN AND DETAILING 16

3.4.1 Columns 16

3.4.2 Floor System 17

3.4.3 Shear Wall 18

4 **NONLINEAR ANALYSES** 20

4.1 INTRODUCTION 20
4.2 SELECTED 2D MODEL 20
4.3 MODELING PARAMETERS 20
4.3.1 General Modeling Parameters 20
4.3.2 Nonlinear Dynamic Analyses Parameters 26
4.3.3 Nonlinear Static Analyses Parameters 28
5 **RESULTS AND OBSERVATIONS** 30
5.1 INTRODUCTION 30
5.2 REPRESENTATIVE RESULTS 30
5.3 SUMMARY OF RESULTS 37
5.3.1 Results from the Nonlinear Dynamic Analyses 37
5.3.2 Results from the Nonlinear Static Analyses 52
5.4 IMPLICATIONS OF RESULTS 62
5.4.1 Elastic Demand versus Realistic Results 62
5.4.2 Realistic Seismic Demand versus Nominal Strengths 62
5.4.3 Allowable Story Drift 64
6 **CONCLUSIONS AND FUTURE WORK** 65
REFERENCES 66

TABLE OF FIGURES

Figure 1: Response Spectra Comparison (5% damped) 12

Figure 2: Plan View of the Floor System 14

Figure 3: Section x-x: Vertical View and Story Heights. 15

Figure 4: Cross-section Detailing of the Columns 16

Figure 5: Column Layout of Typical Longitudinal and Transverse Reinforcement per Story 17

Figure 6: Cross-section Detailing of the Beams 17

Figure 7: Beam Layout of Longitudinal and Transverse Reinforcement 17

Figure 8: Two-way Joist Slab Section Detail 18

Figure 9: Cross-section Detail of the Shear Wall for the First Three Stories 18

Figure 10: Cross-section Detail of the Shear Wall for the Upper Stories (4th and 10th) 19

Figure 11: Plan View of the Selected Frames for the Nonlinear Analyses 21

Figure 12: Configuration of the Frames in the Mathematical Model 21

Figure 13: Representation of a Beam Section Using a Fiber Model 22

Figure 14: Model Used to Test the Distributed Elasticity 23

Figure 15: Distribution of Elastic Bending Moments along the Frame's Girder 24

Figure 16: Pushover Curve for the One-Bay-One-Story Frame 24

Figure 17: Distribution of Ductility Demand over the Different Sections at the Integration Points of the Frame's Beam 25

Figure 18: Location of the Two-point Constraints Applied to the Structure 26

Figure 19: Variation of Modal Damping Ratios with Natural Frequencies 28

Figure 20: Ground Acceleration Time Series. 31

Figure 21: Response Spectrum (5% Damped) Comparison 31

Figure 22: Roof Displacement History 32

Figure 23: Roof Total Acceleration History 33

Figure 24: Normalized Base Shear History 33

Figure 25: Normalized Beam's Moment-Ductility Demand History. 35

Figure 26: Normalized Wall's Moment-Ductility Demand History. 35

Figure 27: Drift Ratio at each Floor Level. 35

Figure 28: Absolute-valued Envelopes of Different Structural Responses. 36

Figure 29: Maximum Acceleration per Floor 38

Figure 30: Maximum Drift Ratio per Floor 39

Figure 31: Normalized Maximum Story Shear 40

Figure 32: Maximum Overturning Moment per Story 40

Figure 33: Maximum Bending Moments -Column 1 41

Figure 34: Maximum Bending Moment -Column 2 42

Figure 35: Maximum Bending Moment -Column 3 42

Figure 36: Maximum Bending Moment -Column 6 43

Figure 37: Maximum Bending Moment -Column 7 43

Figure 38: Maximum Bending Moment -Shear Wall. 44

Figure 39: Maximum Bending Moment -Shear Wall. 45

Figure 40: Maximum Shear Demand -Column 1 46

Figure 41: Maximum Shear Demand -Column 2 46

Figure 42: Maximum Shear Demand -Column 3 47

Figure 43: Maximum Shear Demand -Column 6 47

Figure 44: Maximum Shear Demand -Column 7 48

Figure 45: Maximum Shear Demand -Shear Wall 48

Figure 46: Wall's Ductility Demand Histogram for the 104 Ground Motions - Lower Section. 49

Figure 47: Wall's Ductility Demand Histogram for the 104 Ground Motions - Upper Section..... 50

Figure 48: Column's Ductility Demand Histogram for the 104 Ground Motions. 50

Figure 49: Beam's Ductility Demand Histogram for the 104 Ground Motions..... 51

Figure 50: Pushover Curves. 53

Figure 51: Comparison of the Distribution of the Inter-story Drift Ratios for the Nonlinear Static and Dynamic Analyses. 54

Figure 52: Comparison of the Distribution of the Normalized Shear per Story for the Nonlinear Static and Dynamic Analyses. 54

Figure 53: Comparison of the Distribution of the Overturning Moments for the Nonlinear Static and Dynamic Analyses. 55

Figure 54: Comparison of the Distribution of Bending Moment Demand on Column 1 for the Nonlinear Static and Dynamic Analyses. 56

Figure 55: Comparison of the Distribution of Bending Moment Demand on Column 3 for the Nonlinear Static and Dynamic Analyses. 56

Figure 56: Comparison of the Distribution of Bending Moment Demand (Positive Direction of the Loading) on the Wall for the Nonlinear Static and Dynamic Analyses. 57

Figure 57: Comparison of the Distribution of Bending Moment Demand (Negative Direction of the Loading) on the Wall for the Nonlinear Static and Dynamic Analyses. 57

Figure 58: Comparison of the Shear Demand on Column 1 for the Nonlinear Static and Dynamic Analyses. 58

Figure 59: Comparison of the Shear Demand on Column 3 for the Nonlinear Static and Dynamic Analyses. 59

Figure 60: Comparison of the Sheat Demand on the Wall for the Nonlinear Static and Dynamic Analyses. 59

Figure 61: Curvature Ductility Demand versus Normalized Roof Displacement under Rectangular Load Pattern - Shear Wall. 60

Figure 62: Curvature Ductility Demand versus Normalized Roof Displacement under Rectangular Load Pattern - Column 3. 61

1 INTRODUCTION

1.1 MOTIVATION

The main stimulus for undertaking the research project summarized in this paper stems from the differences found in two sets of design codes with respect to the detailing of particular structural elements. The two sets of design codes referenced above are: 1) ACI 318-05[1], IBC2006[2] and ASCE/SEI 7-05[3] collectively, which are used widely in the United States and around the world and 2) NSR-98[4] which is used in Colombia. The specific differences (that are of interest for this paper) between the two sets of codes are related to the design and detailing of reinforced concrete structures located on intermediate seismic zones and described in these codes to be in *intermediate design categories*. **Appendix B** contains a comparison of the differences between the two sets of codes with respect to the detailing of intermediate moment frames. From this comparison, it was apparent that there was a need to review the detailing requirements in the first set of codes; specifically, the allowance to use ordinary type of reinforced structural walls in buildings constructed within intermediate seismic zones.

Another goal of this research project was to assess the behavior of code compliant structural designs under demands imposed by real case scenarios of seismic hazard as defined in the following sections of this document. The idea is to compare the behavior of a real structure analyzed and designed with the typical approach used in structural design offices –using building codes like the IBC2006 and analysis and design recommendations like the ASCE/SEI 7-05 and the ACI 318-05- and run a series of nonlinear dynamics analysis simulating real seismic scenarios to review the behavior of different structural responses.

1.2 OBJECTIVES AND SCOPE

One of the objectives of this research was to review the behavior of intermediate reinforced concrete structures under defined realistic cases of seismic hazard. A review of the detailing requirements of the ACI-318-05 with regard to Intermediate Moment Resistant Concrete Frames and Ordinary Shear Walls was performed. A verification of the adequacy of this reinforcement detailing in a typical Intermediate-type reinforced concrete structure was assessed through a series of nonlinear dynamic analyses.

---

[1] *"Building Code Requirements for Structural Concrete and Commentary". See [Ref.1]*
[2] *"International Building Code 2006". See [Ref. 2]*
[3] *"Minimum Design Loads for Buildings and Other Structures". See [Ref. 3]*
[4] *"Normas Colombianas de Diseño y Construcción Sismo Resistente". See [Ref.4]*

Another objective was to make a comparison between the structural demands imposed by the seismic loads prescribed by the codes (through a design response spectrum of pseudo accelerations versus periods) and the median demand of a realistic scenario of seismic shaking (a selected bin of 104 ground motions). Comparing simplified case scenarios for design with cases involving realistic estimations of seismic hazard levels is of importance to determine the adequacy of the seismic demands and the required structural characteristics proposed by the codes.

As a complementary objective, a validation of a ground motion selection procedure for the analysis of structures was performed. The recent interest in ground motion selection for the evaluation of structures was the motivation to use one of the methods available and compare its results with the defined realistic demand according to **Section 2.2**.

1.3 ORGANIZATION

The paper will be organized into different sections as outlined below:

Seismic demands are estimated in **Section 2**. Seismic demands are split into three separate subsets. The first set of seismic demands are derived from a large bin of 104 ground motions considered to be the "*true*" realistic seismic hazard level for the specific region. The second set of seismic demands are those proposed by the building codes through a design response spectrum (with a Probability of Exceedance of 10% in 50 years). The third set of seismic demands are scaled ground motions given by a time series selection procedure.

The geometric characteristics of the studied building is found in **Section 3**. The detailing and properties of the structural elements that resulted from the code compliant analyses and design are also found in this section.

Section 4 describes the simplified model and parameters used for the set of nonlinear analyses that were undertaken in order to assess a more realistic behavior of the structure under seismic loading.

The results and observations are summarized in **Section 5**. At the end of the section some implications of the results are drawn as an outcome of the work that has been done in this research project.

Section 6 contains the conclusions to this research and provides some recommendations for future studies.

2 SEISMIC HAZARD ESTIMATION

2.1 INTRODUCTION

Two main sources of seismic demand were used throughout this research as input to calculate structural responses: 1) acceleration time series (ground motions) that were input as uniform excitation at the structural model base and 2) elastic response spectrums used in modal response spectrum dynamic analyses.

The ground motions used were determined by two methods as described in **Sections 2.2 and 2.4** and were used in nonlinear dynamic procedures of analyses; the design response spectrum calculation is described in **Section 2.3** and was used in the elastic analysis to design the structure used in this project.

2.2 SITE LOCALIZATION AND PARAMETERS TO ESTIMATE REALISTIC SEISMIC DEMAND

The structure was chosen to be located in an "Intermediate Seismic Zone" (as classified by IBC 2006). The site location was analyzed to characterize its geological surroundings and to quantify typical seismic parameters associated with an "Intermediate Seismic Zone". The important parameters taken into account to characterize the seismic hazard on the building were:

- ***Distance Range to Seismic Source***: $10 \leq ClsD \leq 30$ [km]
- ***NEHRP Soil Class:*** C and D. $300 \leq Vs_{30} \leq 600$ [m/s]
- ***Magnitude Range:*** $6.25 \leq M \leq 6.75$

The ground motion selection was based on the likely maximum magnitude the fault is capable of producing, the distance from the site to the fault and the site conditions. The Pacific Earthquake Engineering Research (PEER) Center, NGA strong motion database was used for this study. Fifty two pairs of grounds motions were selected as representative of the seismic hazard level of the selected site. These 104 time series were used in the analyses without any type of scaling since the median value of their spectral accelerations matched very closely to the elastic response spectrum proposed by ASCE/SEI 7-05 (assumed to be representative of the seismic hazard of the region).

2.3 CODE BASED SEISMIC DESIGN CRITERIA

As it is done in practice, the definition of the seismic demand for design was calculated using the ASCE/SEI 7-05. This code defines a Maximum Considered Earthquake (MCE) Ground Motion as the de-

mand for which a structure must be designed. The definition of the hazard level is given by contour maps of spectral accelerations at specific periods. The resultant pseudo acceleration spectrum defines a seismic hazard level having a 10% chance of being exceeded in 50 years (PE10%-50yrs).

The seismic ground motion values used to construct the design response spectrum are:

- *Mapped Acceleration Parameters:* **S_s=0.65; S_1=0.18**
- *Site Class:* **C**
- *Site Coefficient:* **F_a=1.15; Fv=1.65**
- *Design Spectral Acceleration Parameters:* **S_{DS}=0.49; S_{D1}=0.19**

Other parameters that are important in defining the seismic demand on the structures are:

- *Occupancy Category:* **I**
- *Importance Factor:* **I=1.0**
- *Seismic Design Category Based on S_{DS}:* **C ($0.33 \leq S_{DS} < 0.50$ and Occupancy Category I)**
- *Seismic Design Category Based on S_{D1}:* **C ($0.133 \leq S_{D1} < 0.20$ and Occupancy Category I)**

The design coefficients and factors for seismic force-resisting systems are:

- Seismic Force-Resisting System: **Intermediate Reinforced Concrete Moments Frames**[5]
- *Response Modification Coefficient:* **R=5.0**
- *Deflection Amplification Factor:* ***Cd=4.5***

2.4 GROUND MOTION SELECTION PROCEDURE FOR NONLINEAR DYNAMIC ANALYSIS

In order to validate the work that is being developed by researchers with respect to ground motion selection for the analysis of structures, a time series selection procedure was applied to the ground motion bin obtained in **Section 2.2**.

The employed procedure scaled the acceleration time series to the design spectrum in order to match any of the following: the spectral acceleration at the fundamental period Sa_{T1}, the Peak Ground Velocity (PGV), or some spectral values Sa over a specific period range. A filtering process of the resulting data is undertaken making use of statistical parameters as well as the deviation from PGV and Sa_{2T} (the design spectral acceleration at twice the fundamental period) and the response modification coefficient R.

The ground motion time series selection procedure is illustrated in ***[Ref. 5]*** and is described to produce "*median first mode nonlinear response given a design event*". As a result of applying the selection method to the selected bin of ground motions, eight time series were selected to analyze the building. The median values of various structural responses were calculated and reported in this research.

[5] The actual lateral load resistant system is formed by the combination of intermediate reinforced concrete moment frames and ordinary "C"-shaped reinforced concrete wall to control drifts.

2.5 RESPONSE SPECTRA COMPARISON

The spectra representing the seismic demand imposed on the building through the different analyses performed is shown in **Figure 1**. There is a good correspondence between the spectrum associated with the median of the selected 104 times series and the design spectrum calculated according to ASCE/SEI 7-05. This indicates that for the particular purpose of the research, the hazard level proposed for "Intermediate Seismic Zones" in building codes is adequately represented by median values of spectral acceleration.

The median response spectrum calculated using the eight scaled time series from **Section 2.4** matches the design spectrum at Sa_{T1} and also exhibits similar shape characteristics.

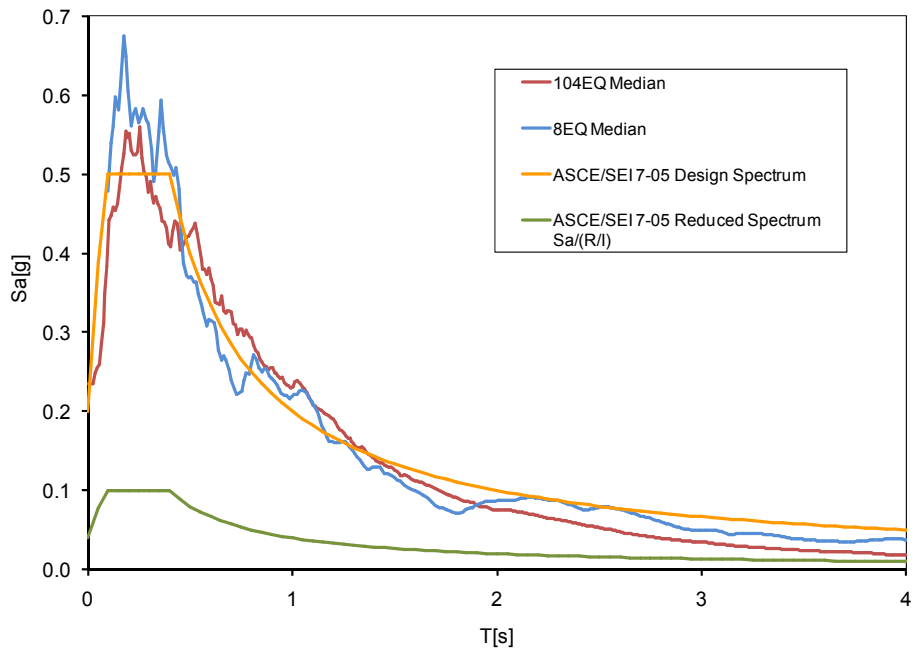

Figure 1: Response Spectra Comparison (5% damped). Shown are median spectral values for the selected 104 and 8 ground motions. The code-based spectra are for a PE-10%-50yrs.

3 STRUCTURAL MODEL

3.1 INTRODUCTION

The selected structure represents a typical structural system used widely in northern South America. The system is composed of moment resisting frames in the longitudinal and transverse directions. The frames are part of both the vertical and lateral load resistant systems and are attached together (as a tridimensional structure) through a rigid diaphragm which is composed of a two way joist slab with beams.

A ”C”-shaped reinforced concrete wall was added to the system in order to limit the maximum drift ratio to less than 1%. The latter was done to comply with a reasonable limitation found in reference building codes such as NSR-98.

These types of combined systems (with lateral load resisting frames in both directions) tend to be very redundant and to a good extent (if properly designed) safe in the event of strong lateral shaking.

3.2 GEOMETRIC DESCRIPTION AND MATERIAL’S STRENGTH

3.2.1 Structures’ Geometry

The following are the typical structural characteristics of the building used throughout this project:

- *Structural System*: **Intermediate Moment Resistant Concrete Frames and Ordinary Reinforced Concrete Shear Walls**[6]
- *Number of stories:* **10**
- *First Floor Height:* **10’-6”**
- *Typical Height (center to center):* **9’-2”**
- *Total Height:* **93’**
- *Floor System:* **Two Way Joist Slab with Beams**
- *Structural Area per Floor:* **4.680ft^2**
- *Span Ranges (center to center):* **9’-10” to 19’-8”**
- *Beam and Joists Dimensions:* **Joists ➔ 8”x16”**
  Beams ➔ 16”x16”
- *Columns Dimensions:* **20”x20” ; 20”x28”**
- *Wall Thicknesses:* **8” (1st, 2nd and 3rd story)**
  6” (4th to 10th story)

[6] The shear walls were introduced in the building to control the maximum drift ratio under 1%.

Figure 2 and 3 show a typical floor plan and a longitudinal section cut of the story heights

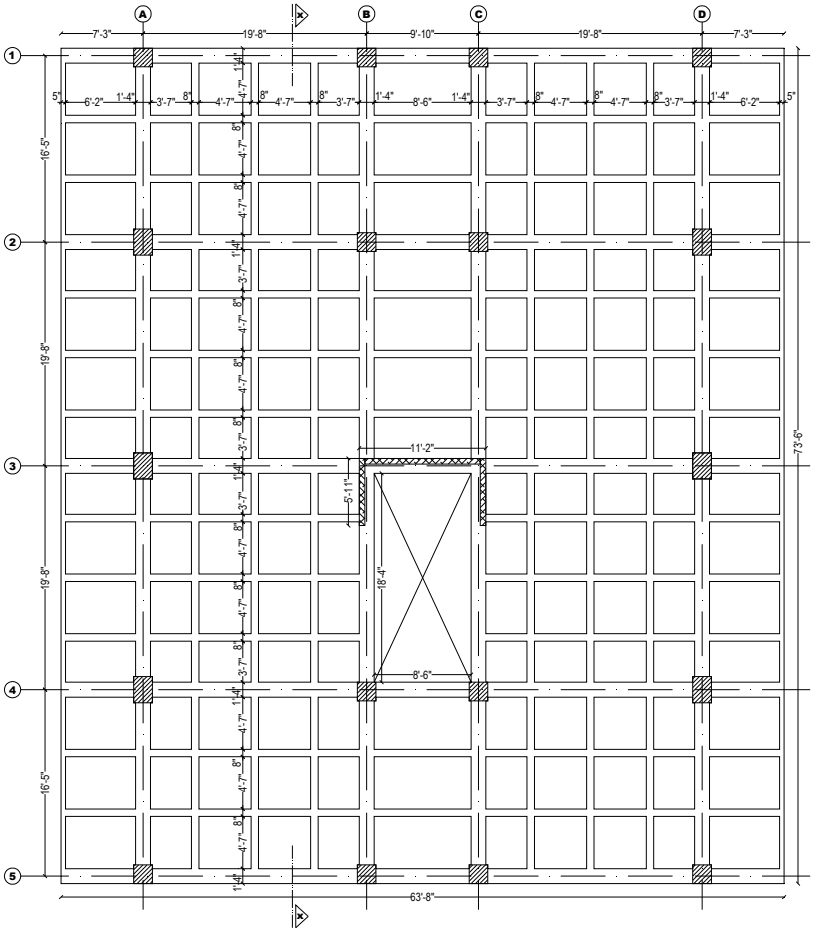

Figure 2: Plan View of the Floor System

3.2.2 Selected Materials

The nominal properties of the materials selected for the structural elements are as follows –normal weight concrete was assumed-:

- *Floor system:* **f'c = 3.000psi**
  Ec = 57.000(f'c)$^{1/2}$=3'122.019psi

- *Columns and Walls:* **f'c=4.000psi**
  Ec = 57.000(f'c)$^{1/2}$=3'604.997psi

- *Reinforcement:* **fy=60.000psi**

3.3 ELASTIC ANALYSIS

The structural analysis was based on Chapters 11 and 12 of ASCE/SEI 7-05 and IBC2006 Chapter 16. A modal response spectrum analysis was performed in order to determine the seismic demand on the structural elements.

The computer model used for the analysis considered cracked section moment of inertia properties of the elements to account for cross sectional degradation due to ultimate vertical load conditions and the assumed lateral demand. The mass of the elements was lumped in each floor and the structural elements at each story were attached by a rigid diaphragm constraint. **Appendix A** contains all the relevant data regarding the elastic analysis (i.e. modeling parameters, load combinations, seismic demand calculations, etc.) as well as the response resulting from the linear elastic modeling of the structure (i.e. modal analysis output, accidental torsion analysis, drift ratios estimations).

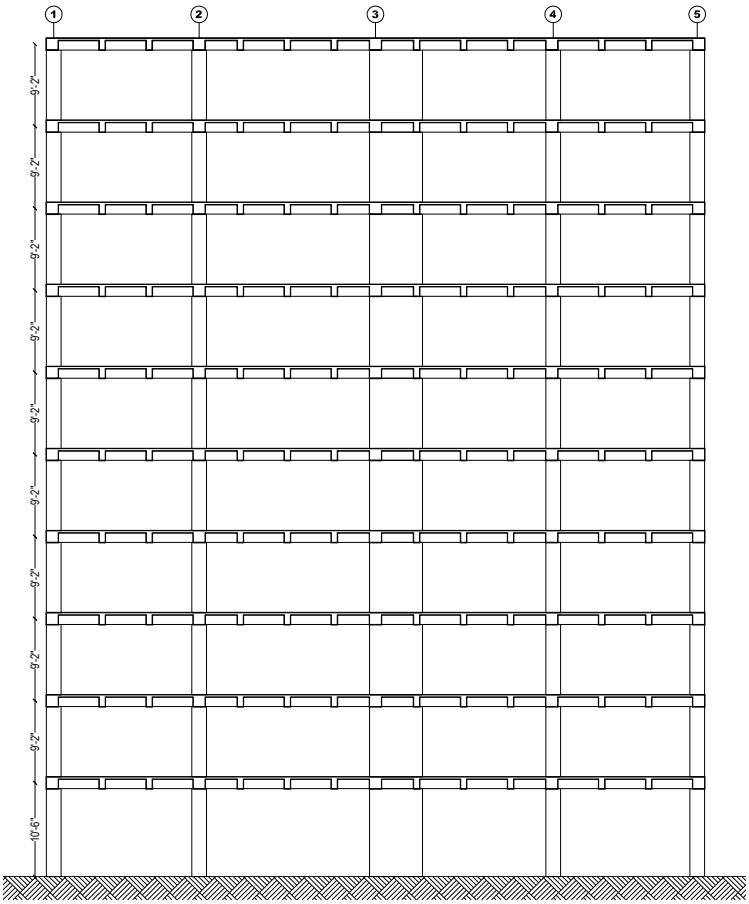

Figure 3: Section x-x: Vertical View and Story Heights.

3.4 DESIGN AND DETAILING

With the results obtained from the analysis, the design was undertaken following the recommendations of ASCE/SEI 7-05 Chapter 14 and IBC2006 Chapter 19. The design procedure was based on the ACI 318-05 code Chapters 1 through 18. For the detailing of the Intermediate Moment Resistant Concrete Frames, recommendations from Chapter 21 were followed and references from the NSR-98 were used[7].

The detailing requisites for Intermediate Moment Resistant Concrete Frames are given by ACI 318-05 Chapter 21.12 "Requirements for intermediate moment frames". It was found that the design was governed by minimum requirements with respect to the shear detailing of the beams and for the longitudinal and shear reinforcement of the columns. The shear walls were detailed as Ordinary Structural Walls as recommended by IBC2006 Chapter 1908.1.4 and ACI 318-05 Chapter 21.2.1.3.

3.4.1 Columns

Figures 4 and 5 show typical cross sections of the design columns and the layout of horizontal and longitudinal reinforcement respectively. The spacing and detailing of the transverse steel was dictated by minimum requirements according to Chapter 21.12.5 of the ACI 318-05 code.

The steel quantity for the longitudinal reinforcement ranged from ρ=1% to ρ=1.7%. The small amount of reinforcement steel is explained by three factors: 1) the uniform distribution of vertical load over all the frames through the use of a two way slab system, 2) the large cross section of the columns required to control drifts, and 3) the intermediate seismic demand proposed by the analysis code.

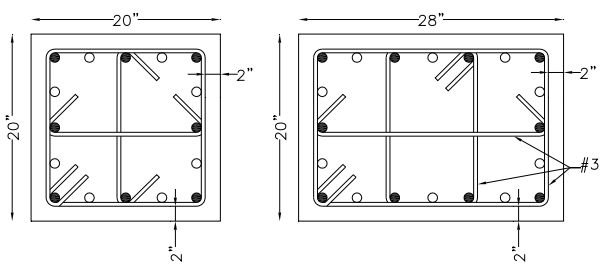

Figure 4: Cross-section Detailing of the Columns

[7] Appendix 2 contains a comparison of the requirement proposed by ACI 318-05 and the reference code NSR-98 with regard to the detailing of Intermediate Reinforced Concrete Moment Frames.

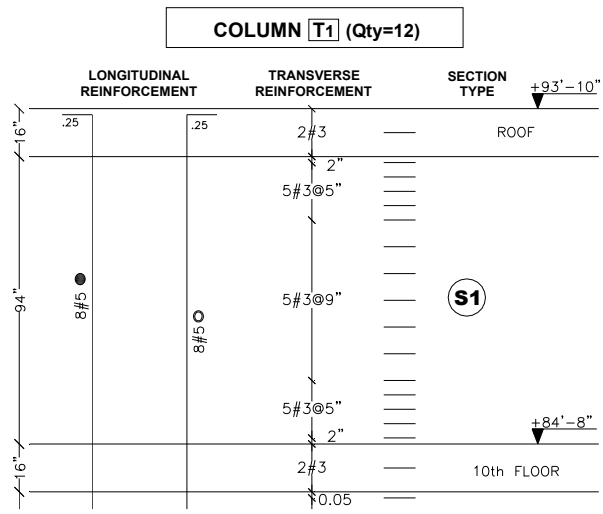

Figure 5: Column Layout of Typical Longitudinal and Transverse Reinforcement per Story

3.4.2 Floor System

Figures 6, 7 and 8 depict the typical detailing used for the elements of the floor system. This system can be described as a two way joist slab with beams. For the purpose of the analysis, the system is considered fully rigid in the in-plane direction. The detailing of the beams was performed following the recommendations of Chapter 21.12.4 of the ACI 318-05.

Due to the characteristic distribution of vertical load over all the frames, the steel quantities range from the minimum allowed quantity of ρ=0.35% to ρ=0.80%. The fact that the quantities of longitudinal reinforcement are under ρ=0.9% is a good indication of the behavior of the system under service loads with respect to vertical load related deflections.

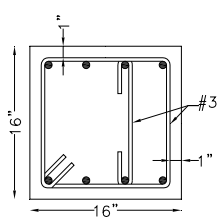

Figure 6: Cross-section Detailing of the Beams

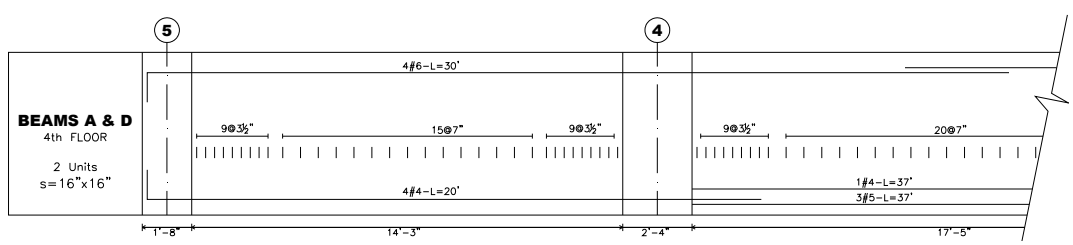

Figure 7: Beam Layout of Longitudinal and Transverse Reinforcement

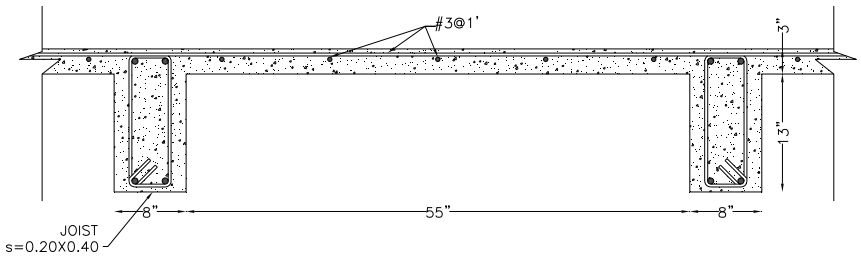

Figure 8: Two-way Joist Slab Section Detail

3.4.3 Shear Wall

With the purpose of stiffening the lateral load resisting system of the building, a ”C”-shaped shear wall was accommodated close to the geometric center of the footprint. **Figures 9 and 10** show the detailing of the two types of shear walls used over the building height. Following the recommendations of Section 1908.1.4 of the IBC-2006, these elements were designed as ordinary reinforced concrete walls according to Chapter 14 – Walls of the ACI 318-05.

Unlike the columns, demands on the walls in the first three stories of the structure were considerable. Therefore, boundary elements and a higher quantity of longitudinal (vertical) as well as transverse (horizontal) reinforcement steel were required. The maximum vertical and horizontal steel quantity was ρ_ℓ=0.90% and $\rho_{\ell\,\mathbf{min}}$=0.25% for walls in the first three stories. In the upper walls (4th story and up), maximum longitudinal and transverse steel quantities were ρ_ℓ=0.33% and $\rho_{\ell\,\mathbf{min}}$=0.20%.

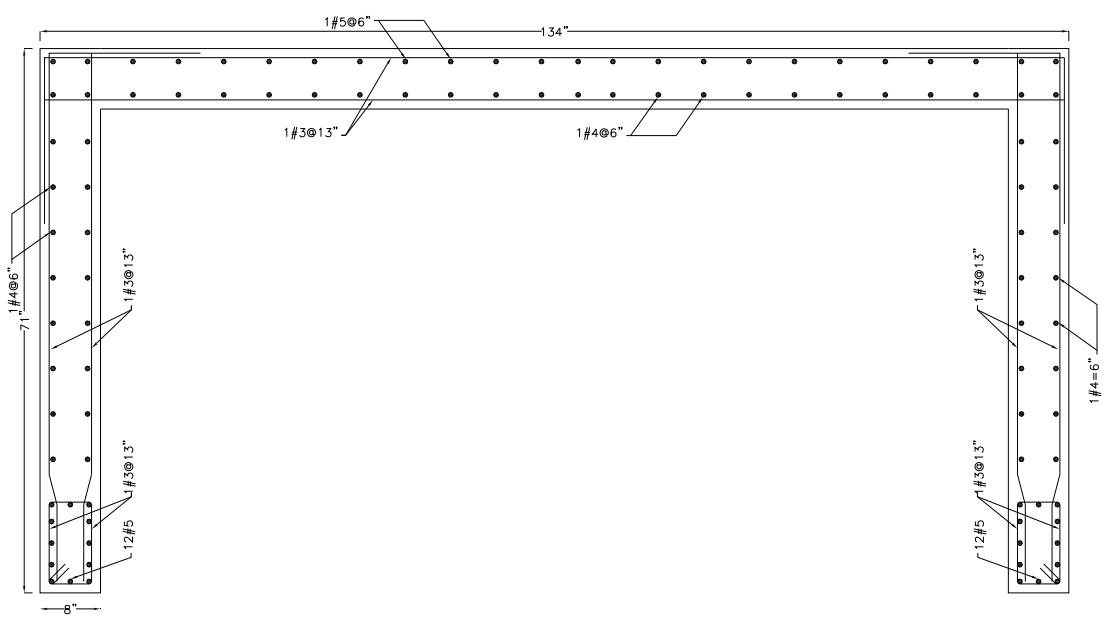

Figure 9: Cross-section Detail of the Shear Wall for the First Three Stories

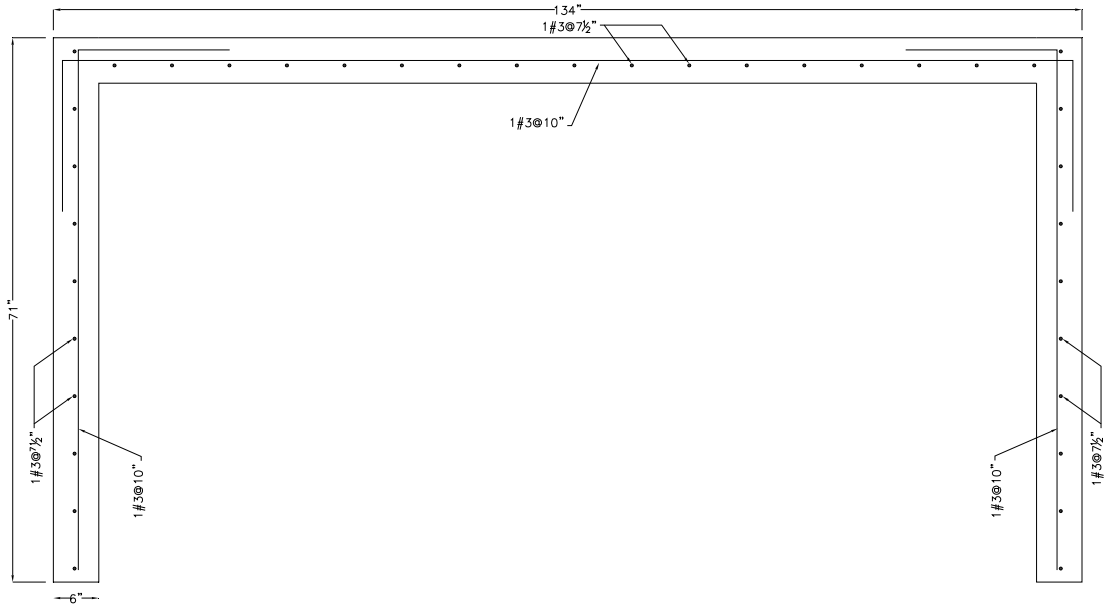

Figure 10: Cross-section Detail of the Shear Wall for the Upper Stories (4th and 10th)

4 NONLINEAR ANALYSES

4.1 INTRODUCTION

As one of the most powerful tools available to model the actual behavior of structures under time varying lateral loads, nonlinear types of analyses were utilized throughout the research in order to obtain various structural response values of interest. The Open System for Earthquake Engineering Simulation (OpenSees)[8] was selected as the modeling tool because the nonlinear analyses capabilities of the software have been validated by many researchers. OpenSees Navigator[9] was the preferred interface used to input the model and to collect the resulting data from the analyses. ***[Ref. 6]*** contains all the pertinent documentation on how to implement the structural modeling on OpenSees and ***[Ref.7]*** contains information about OpenSees Navigator.

4.2 SELECTED 2D MODEL

With the purpose of avoiding excessive time consumption and to focus on a few important parameters in the modeling phase of the research, a two dimensional model representative of the structure was chosen to be analyzed. As it is shown in **Figure 2**, the symmetric geometry of the building made possible the selection of half of the vertical and lateral load resistant system in the longitudinal direction (frames A and B with half of the wall's section). These two frames, along with the corresponding shear wall, were modeled in parallel through a rigid diaphragm constraint and assumed to give a representative behavior of the entire structure. **Figure 11** shows a plan view of the selected frames and **Figure 12** the corresponding representation of the bi-dimensional model.

4.3 MODELING PARAMETERS

4.3.1 General Modeling Parameters

Two types of nonlinear analysis were performed on the building: 1) Nonlinear Dynamic Analysis and 2) Nonlinear Static Analysis (Pushover). **Sections 4.3.2 and 4.3.3** contain, respectively, all the pertinent data corresponding to the two options used in the analyses mentioned above.

[8] http://opensees.berkeley.edu
[9] http://peer.berkeley.edu/OpenSeesNavigator/

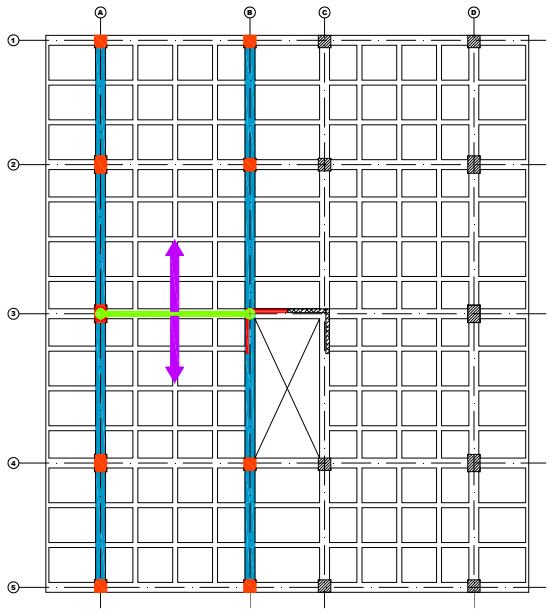

Figure 11: Plan View of the Selected Frames for the Nonlinear Analyses

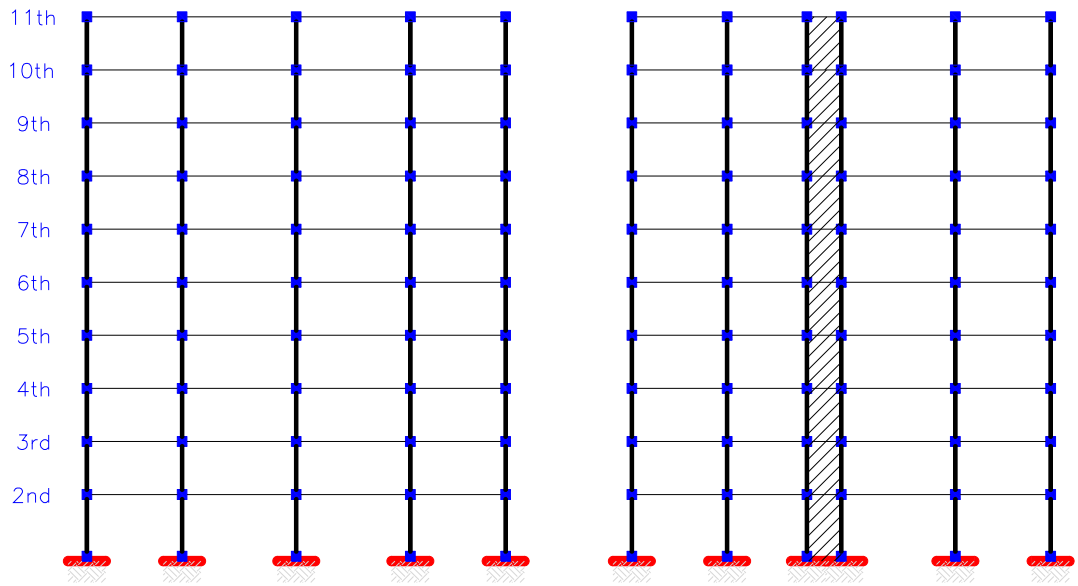

Figure 12: Configuration of the Frames in the Mathematical Model

Though in the following sections there is some specific information regarding the two types of analysis performed, some general modeling parameters of importance were shared by all the analyses and are as follows:

Materials Used

UNIAXIAL materials were used throughout the analyses in OpenSees. This type of object defines a uniaxial stress-strain relationship for each material. The specific stress-strain relationships as well as other behavioral properties were defined according to the expected actual values of materials used in the design (where nominal values were assumed).

In OpenSees, *CONCRETE02* was used to model the unconfined as well as the confined concrete. Chapter 14 of ***[Ref. 6]*** contains all the pertinent data with regard to the material parameters. The STEEL01 material was used to model the assumed bilinear behavior (with strain hardening) of the reinforcement steel. Chapter 16 of ***[Ref. 6]*** contains the material parameters used to recreate the rebar behavior in tension and compression.

Section Types

Fiber sections were used to represent the realistic behavior of the element sections. Each fiber was assigned one of the materials defined previously and is able to trace its corresponding stress-strain relationship. For the analyzed structure, fibers were "patched" to the sections to represent confined and unconfined concrete as well as reinforcement steel layers. **Figure 13** shows how a fiber model represents an actual beam section.

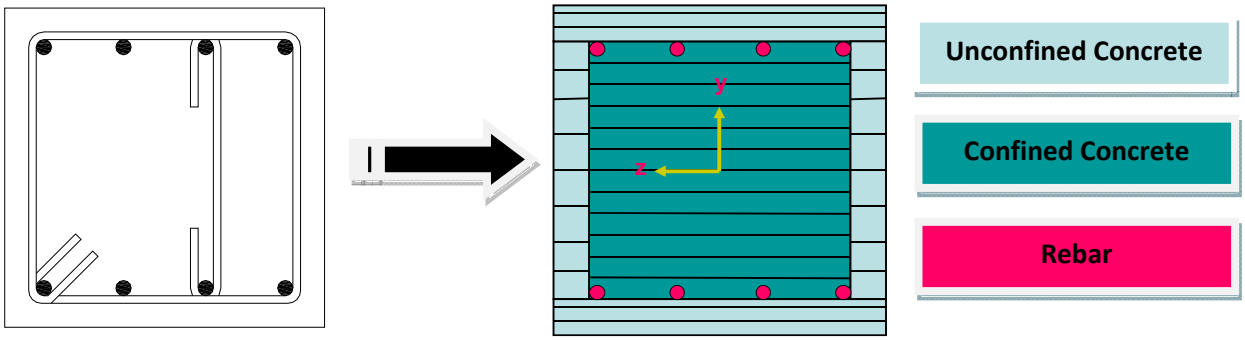

Figure 13: Representation of a Beam Section Using a Fiber Model

Appendix C contains the different sections responses of the elements used in the mathematical model.

Distributed Plasticity

Due to intermediate gravity and lateral load demands on the structural elements, it was decided that a distributed plasticity model was an appropriate assumption to capture the behavior of the horizontal and vertical structural members under the action of vertical and lateral loading. This method was adopted to be able to capture plastic zones at regions away from the beam ends due to the relatively high ratio between gravity and seismic demands.

In order to test the ability of the model to capture plastic hinges forming outside of the beam end locations a one-story one-bay frame was pushed into the nonlinear range and the results for the moment-curvature relations for the beam were recorded for each section. **Figure 14** describes the geometry of the frame tested, where the distributed loads applied and the beam dimensions are the same to those used in the building elastic design. The sections used are also the same as the ones used in the design of the building. The right hand side of **Figure 14** shows the distribution of the fiber sections along five integration points (5IP) for the beam; an elastic section was used for the columns. It is worth mentioning that the quantity (ρ) of the bottom and top steel are proportional to the elastic demand in bending and because of that, the moment capacities are different for positive or negative curvatures –being smaller for positive moment.

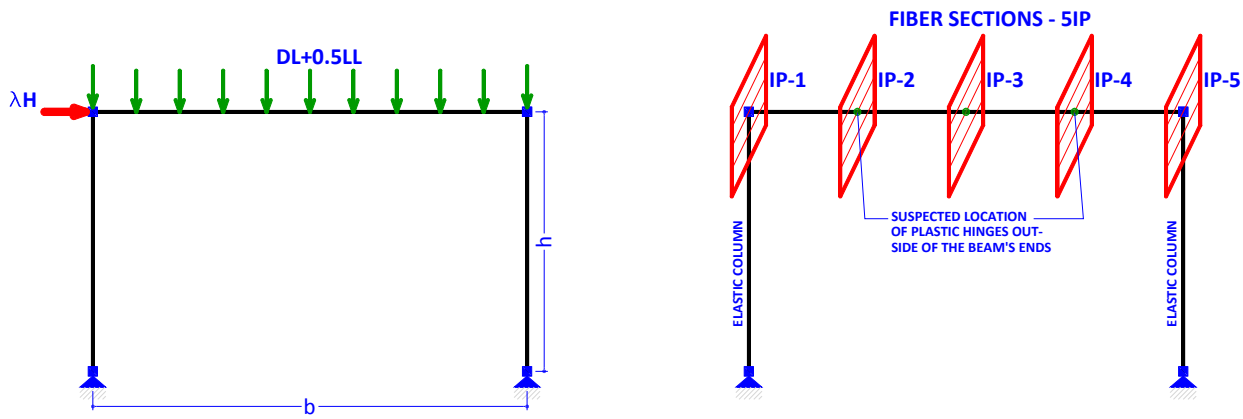

Figure 14: Model Used to Test the Distributed Elasticity

Figure 15 shows that for a combination of vertical and lateral load, the positive bending moment region induced by gravity alone shifts from the center of the girder toward one of the ends. The "shift" in the location of the maximum bending moment and the increase of its value may overstress some sections over their elastic capacity limit for bending. For the particular frame used, sections located about ¼ span length of the beam (near location IP-2) might experience this extra demand and thus a concentration of deformation.

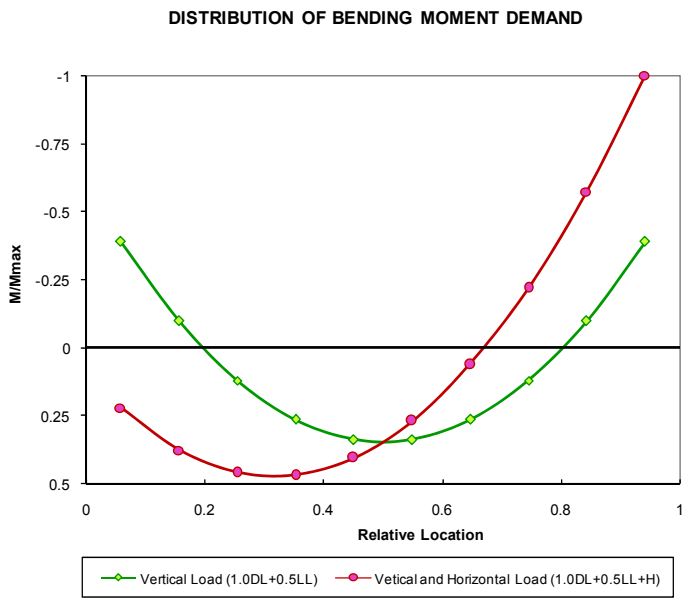

Figure 15: Distribution of Elastic Bending Moments along the Frame's Girder

Figure 16 contains the pushover curve for the frame when pushed to a drift ratio of 3%. **Figure 17** contains the ductility demand at each of the five integration points of the girder. It can be observed that the sections that underwent nonlinear deformations were sections at IP-2 and IP-5. the largest ductility demand occurred at IP-5, where the elastic bending moment demand was more than twice of that close to IP-2(see Figure 15).

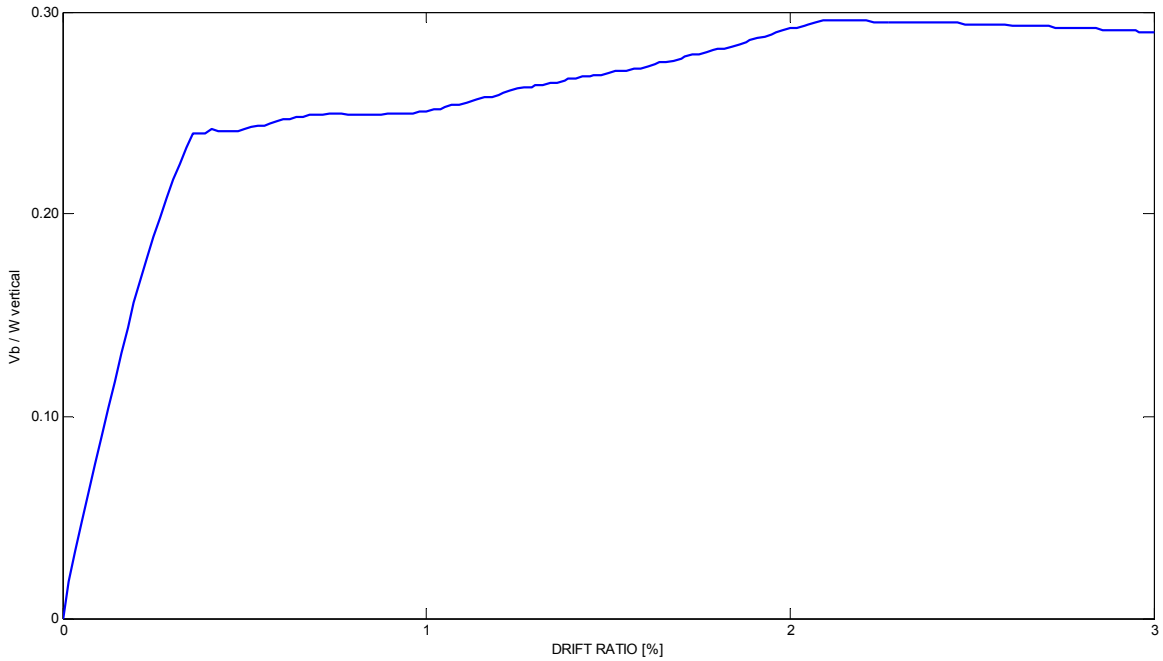

Figure 16: Pushover Curve for the One-Bay-One-Story Frame

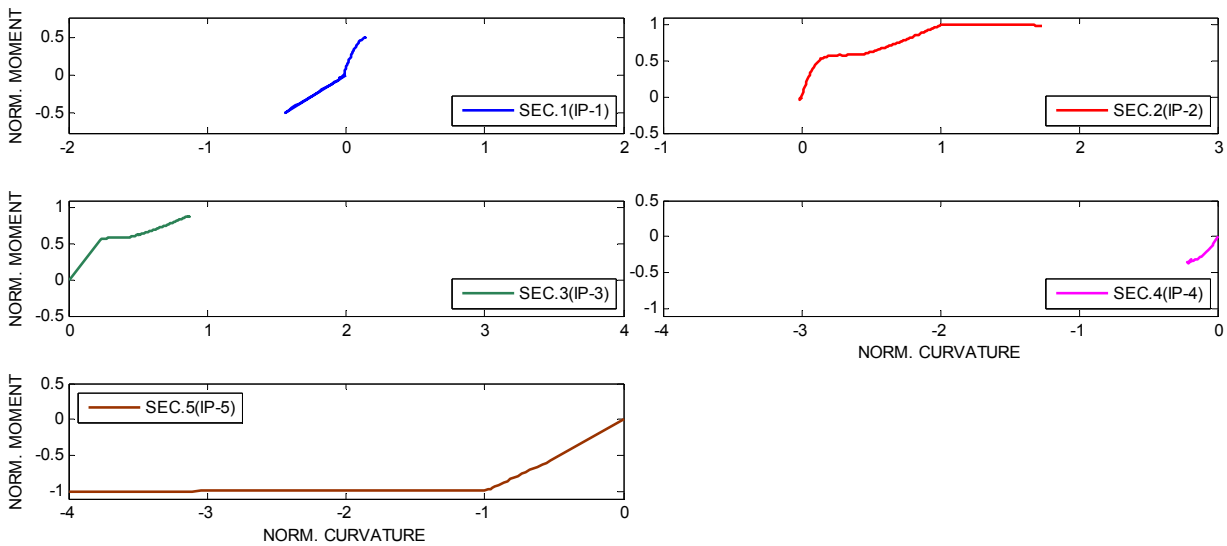

Figure 17: Distribution of Ductility Demand over the Different Sections at the Integration Points of the Frame's Beam

The results shown on **Figure 17** demonstrate that the distributed plasticity model is adequate to represent the moment-curvature behavior of the elements at any section of the span's length. For the particular building analyzed in this paper, situations of extra demand imposed over already "opened hinges", at sections away from the beams ends, should not be of concern since the permanent vertical deformation –deflection- in the beams is of negligible magnitude due to the intermediate vertical and seismic load demand; the low steel quantity supports the latter observation.

Rigid Diaphragm Constraint

The large in plane stiffness of the floor system was taken into account by assuming a rigid diaphragm, modeled by constraining the frame joints. Due to this assumption and the symmetry of the building, a parallel model of two frames was used to represent to the behavior of the structure in the longitudinal direction.

To avoid numerical problems when performing the nonlinear analyses, only two-point constraints were used to tie the horizontal displacements of the frames in the 2D model. The large axial rigidity of the beams permitted the assumption that the joint displacements in the horizontal direction within each frame were equal. Shown in **Figure 18** are the locations of the horizontal constraints applied to the structure.

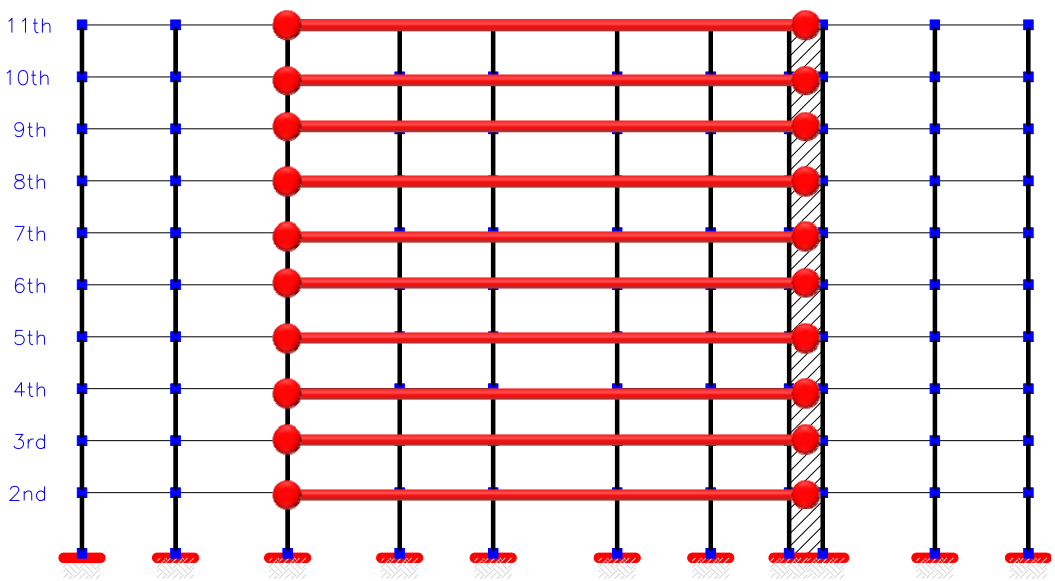

Figure 18: Location of the Two-point Constraints Applied to the Structure

Geometric Transformation

In order to transform the element stiffness and resisting forces from the basic local system to the global coordinate system, two different geometric transformations were enforced throughout the analyses. P-Delta type of geometric transformation was used for the columns while linear geometric transformation was used for the beams. The P-Delta geometric transformation takes into account second order P-Delta effects when transforming the elements' stiffness and resisting force. The small target drift ratio of $\Delta \leq 1\%$ used in the elastic design of the structure leads to a reasonable assumption that an elastic geometric transformation is valid for the beams.

4.3.2 Nonlinear Dynamic Analyses Parameters

The following were the parameters and structural characteristics used during the series of dynamic nonlinear analyses performed using OpenSees and OpenSees Navigator:

- ***Analysis Type: Transient Nonlinear***. This type of analysis uses a time stepping procedure to obtain discrete states of the response of the analytical model. The general equation for transient equilibrium is given by $F_I(\ddot{U}) + F_R(U, \dot{U}) = P(t)$. Where F_I represents the inertial force vector, F_R represents the displacement-dependent (stiffness) and velocity-dependant (damping) resisting-force vector. The external applied force is given by $P(t)$.
- ***Constraint Handler Type: Transformation Method.*** The constraint handler determines how the constraint equations are enforced in the analysis. The degrees of freedom (DOF) in the structure can be separated as follows:

$U = \begin{pmatrix} U_R \\ U_C \end{pmatrix}$, where U_R represents the retained DOFs and U_C the condensed ones.

The Transformation Method transforms the stiffness matrix by condensing out the constrained DOFs. In this case, the constraint equation can be written as: $(T^T K T^T) U_R = T^T R$; where K is the stiffness matrix, U represents the DOF, R is the resisting force and T is the transformation matrix.

- ***Integrator Type: Newmark*** with β=0.25 and γ=0.50. The structure is assumed classically damped.

  The mass-proportional and stiffness-proportional Rayleigh Damping ($c = a_0 m + a_1 k$) was used to simulate the energy dissipation characteristics of the building. For a damping ratio ζ=5% for the first and third elastic modes, the mass proportional and stiffness proportional coefficients are a_0=0.2605 and a_1=0.0037 respectively. **Figure 19** represents the variation of the damping ratios with respect to the modal natural frequencies of the analyzed structure.

- ***Solution Algorithm Type: Modified Newton Algorithm.*** The Newton-Raphson method is used to advance from one step to the next. The tangent stiffness of the system is not updated at each step to avoid expensive calculations with the cost of an increase in the number of iterations to reach a predetermined accuracy level.

- ***Convergence Test Type: Energy Increment Test.*** A convergence test is required by the solution algorithm to determine if convergence has been achieved at the end of an iteration step. The convergence test is applied to : $K \Delta U = R$.

  The Energy Increment Test performs the following check: $1/2\,(\Delta U^T R) < tol$.

- ***DOF Numberer Type: RCM.*** The DOF numberer relates equation number to degrees-of-freedom. Specifically, the RCM numberer uses the Reverse Cuthill-McKee algorithm which optimizes the node numbering to reduce bandwidth and therefore computational time.

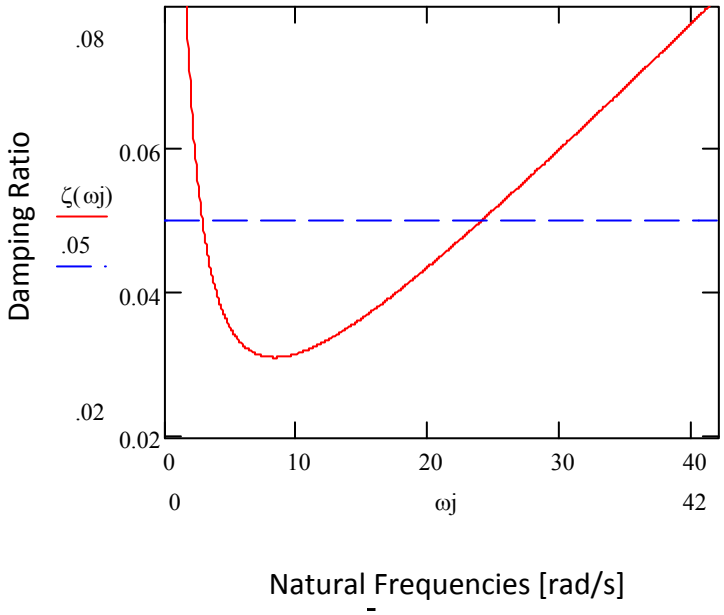

Figure 19: Variation of Modal Damping Ratios with Natural Frequencies. Rayleigh Damping a0=0.2605 and a1=0.0037

- ***System of Equations Type: Band General.*** This feature is used to construct the linear system of equations (LinearSOE) and LinearSolver to store and solve the system of the equations in the analysis. The Band General system constructs an un-symmetric banded system of equations that will be factored and solved using the Lapack band general solver.

4.3.3 Nonlinear Static Analyses Parameters

Four pushover analysis curves were constructed through nonlinear static analyses of the structure: 1) pushover curves for both directions pushed with a rectangular shape pattern load and 2) pushover curves for both directions pushed with a first-mode-shape load pattern.

The following are the parameters that were modified from **Section 4.3.2** "Nonlinear Dynamic Analyses Parameters" to handle the Nonlinear Static Analyses:

- ***Analysis Type: Static***. This type of analysis solves the $KU = R$ problem without the contribution of the mass or the damping of the system. A convenient way to write the equilibrium equations at each step is $R(U) = \lambda P - F_r(U)$ where λP is the factored applied load pattern and F_r represents the displacement-dependent (stiffness) resisting-force vector. At each increment of the load factor λ equilibrium is given by $R(U) = 0$.

- ***Integrator Type: Displacement Control.*** Defines the displacement step increment at which the structure is going to be moved from one state to the next. The resisting forces resulting from each displacement are related to the load factor, λ as described before.

5 RESULTS AND OBSERVATIONS

5.1 INTRODUCTION

In this section, a summary of the results obtained throughout the research project are presented. As an introduction, the first part of the chapter presents typical responses recorded for different levels of shaking; this section helps to understand the general behavior of the structure under various levels of seismic demand.

Then, the structural responses related to the different seismic demands, described in **Section 2**, are presented. In general, the responses of the 104 times series of **Section 2.2** is shown along with its median values, the median values of the selected 8 ground motions from **Section 2.4** and the elastic demand.

As a complementary outcome, results from the pushover analyses are presented. The intention is to show the behavior of structural elements at different levels of displacement demand for the structure.

5.2 REPRESENTATIVE RESULTS

Three ground motions were selected from the bin of the 104 time series and some representative results gathered from the nonlinear dynamic analysis are shown next. The selected ground motions identifications are: EQ75, EQ66 and EQ81 which represent low, intermediate and high level of shaking respectively.

Figures 20 and **21** are a comparison of the three acceleration-time series and their respective response spectrum (5% damped) developed from each.

In these figures the level of shaking is represented by the different values of ground acceleration and pseudo acceleration spectral coordinates. It is apparent that larger levels of lateral shaking (i.e. EQ81<EQ66<EQ75) have larger values of ground acceleration in the time series and higher spectral acceleration values in the short period (high frequency) range of the response spectrum. It is worth mentioning that the spectral accelerations that correspond to the equivalent elastic fundamental period of the nonlinear model (i.e.$T_1 \approx 1.80$s) are accordingly related to the level of shaking (PSa_1EQ75< PSa_1EQ66< PSa_1EQ81); the latter holds for periods T>1.40s.

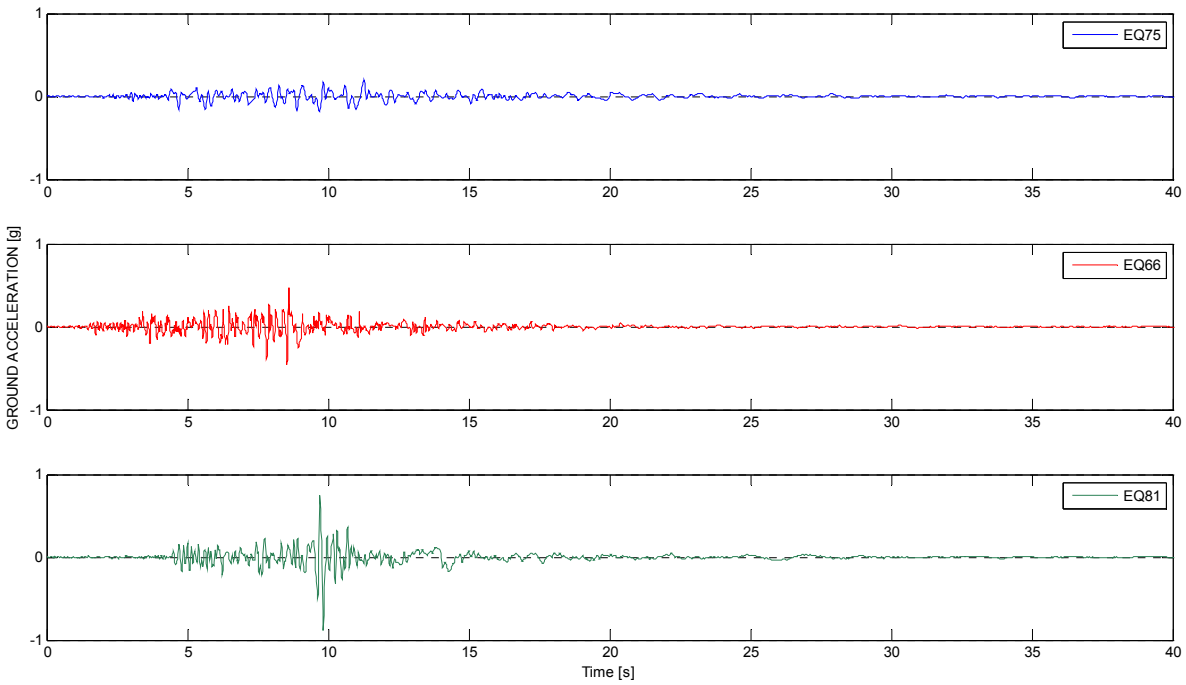

Figure 20: Ground Acceleration Time Series.

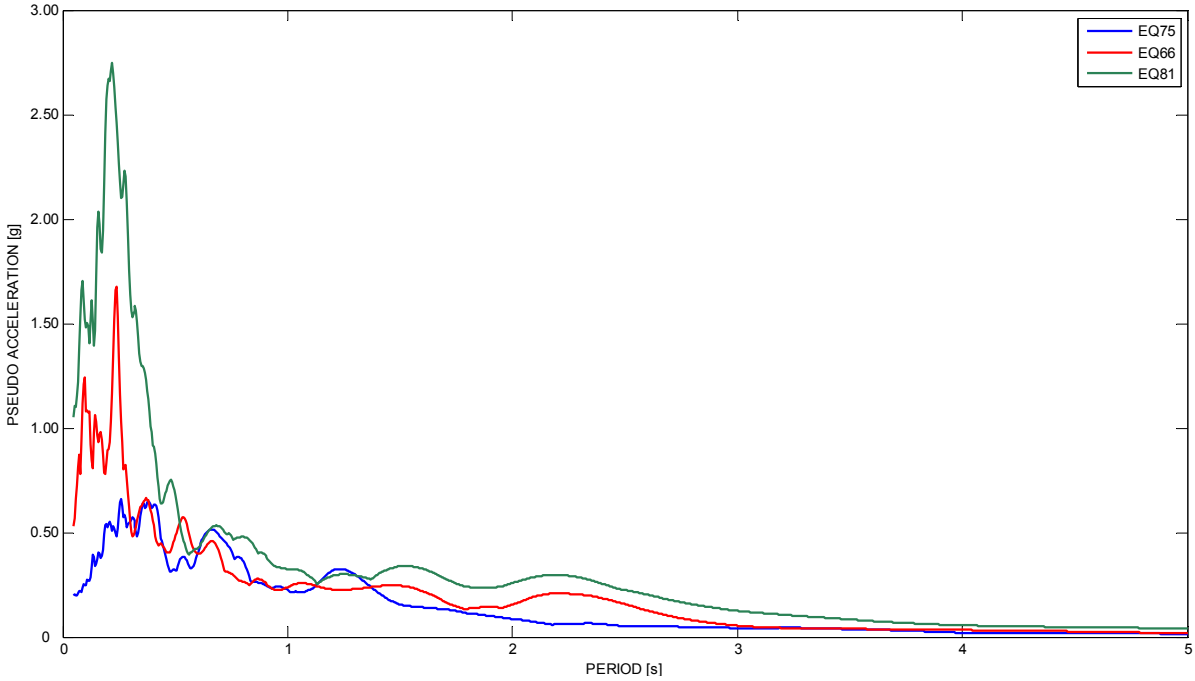

Figure 21: Response Spectrum (5% Damped) Comparison

Figures 22 to **28** show different structural responses which were gathered for each of the three ground motions referenced above. These figures also represent the type of data acquired for each one of the 112 dynamic analyses performed (104 analyses for the bin described in **Section 2.2** and 8 for the ground motions selected in accord with **Section 2.4**) and is summarized in **Section 5.3.1**.

The roof displacement histories depicted in **Figure 22** show a quasi stable displacement pattern of the roof. The sinusoidal-like shape, cycles back and forth with a period ranging from 2.0 to 2.5s; these values are slightly higher than the fundamental elastic period of the structure and correspond to a period related to a degraded stiffness of the structure. It is observed that EQ81 imposes a permanent offset in the displacement history of the roof; the latter is a response to the larger ductility demand imposed in the structural elements.

The acceleration histories reported in **Figure 23** correspond to the amplified values of roof acceleration with respect to the ground motion. The amplification factors for the presented results are 2.07, 1.22 and 1.31 for EQ75, EQ66 and EQ81 respectively.

The base shear time histories (normalized to the total weight of the structure), are presented in **Figure 24**. It can be observed that the different levels of shaking are not linearly related to the measured base shear. This is a consequence of the upper bound limit imposed by the bending moment capacity of the structural elements (i.e columns and wall) and demonstrates the nonlinear behavior of the structure.

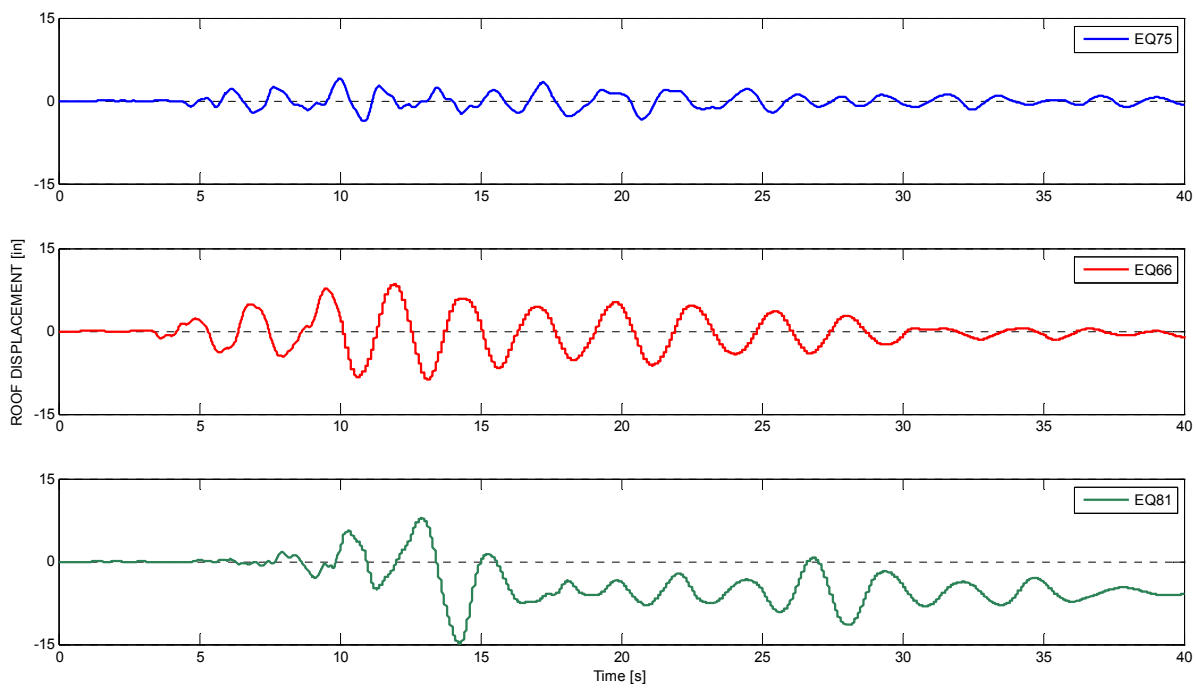

Figure 22: Roof Displacement History

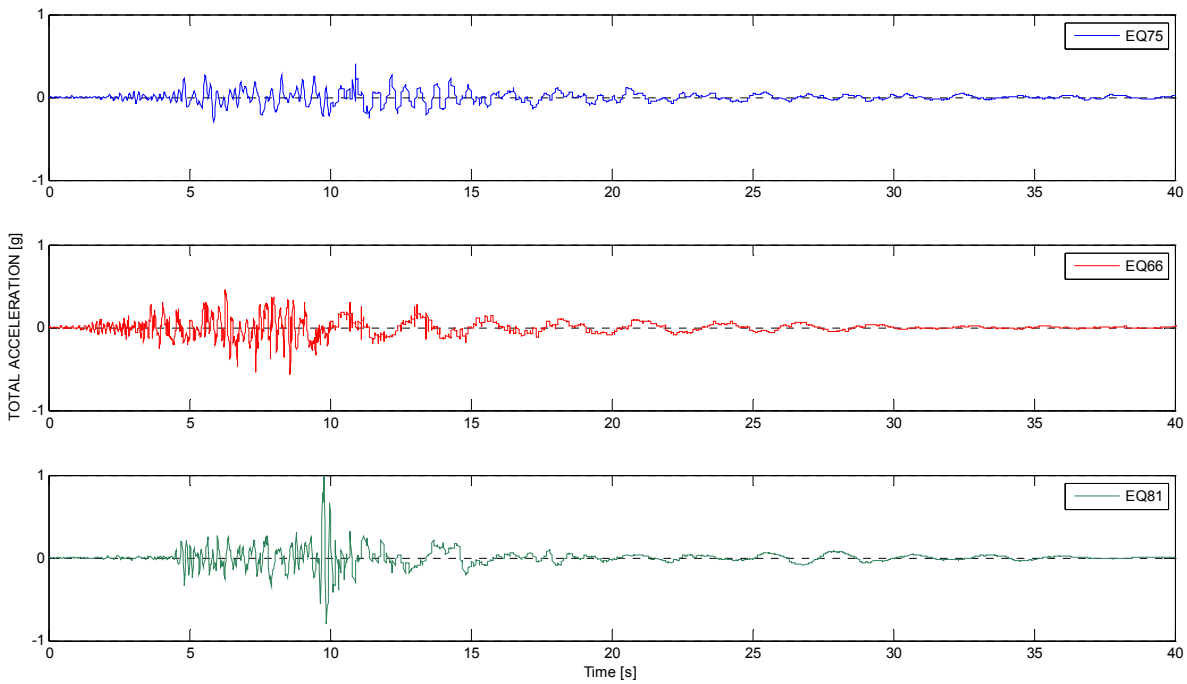

Figure 23: Roof Total Acceleration History

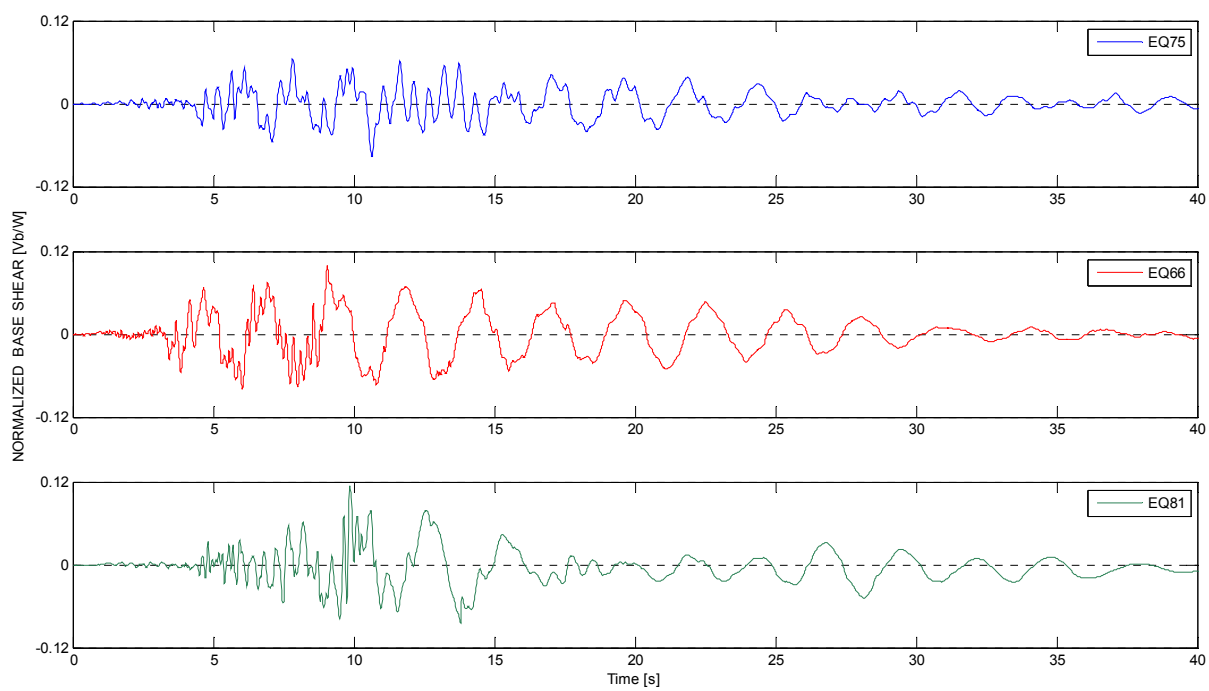

Figure 24: Normalized Base Shear History

Figure 25 shows plots of normalized curvature ductility demand ($\mu = \phi/\phi_{yield}$) versus normalized bending moment (M/M_{pr}). The results shown are for the left end (i.e. first integration point IP-1) of a randomly selected beam on the 5th floor. It is observed that for the three demand levels, the beam yields in only one direction due the demand imposed by gravitational loads. Though for EQ66 and EQ81 there is a reversal in the bending moment demand, the level of shaking is never larger enough to make the beam yield in both directions. Another observation that can be made is that the ductility demand in the beams is proportional to the intensity of the seismic demand ($\mu_{ult,EQ81} > \mu_{ult,EQ66} > \mu_{ult,EQ75}$).

In **Figure 26** analogous results are presented for the bottom of the wall (IP-1) in the first story of the building. The low level of shaking intensity represented by EQ75 does not demand the portion of the wall shown into the nonlinear range, though it does show the cracking that takes place when the ends of the element are demanded in tension. A pinched hysteretic behavior is shown for all three time series. With EQ66 and EQ81 it is demonstrated that larger shaking intensities demand the wall to ductility values larger than the yielding curvature. It is shown how the fiber model proposed for the wall is able to capture the non-ductile behavior of the moment-curvature relationship. When the web of the wall is compressed to large enough strains, a rapid decay in moment capacity for increasing values of curvature demand is promoted; the latter is evident in the positive quadrant of the graph where ductility demand values of five are reached.

The inter-story drift ratio curves are shown in **Figure 27**. Shown in solid lines are the envelopes of the drift ratio history for the different seismic demands. The dashed lines represent drift ratio values at randomly selected times in the displacement history. In this set of graphs, the building responses are proportional to the seismic demand because there is no upper limit for the displacements of the structure.

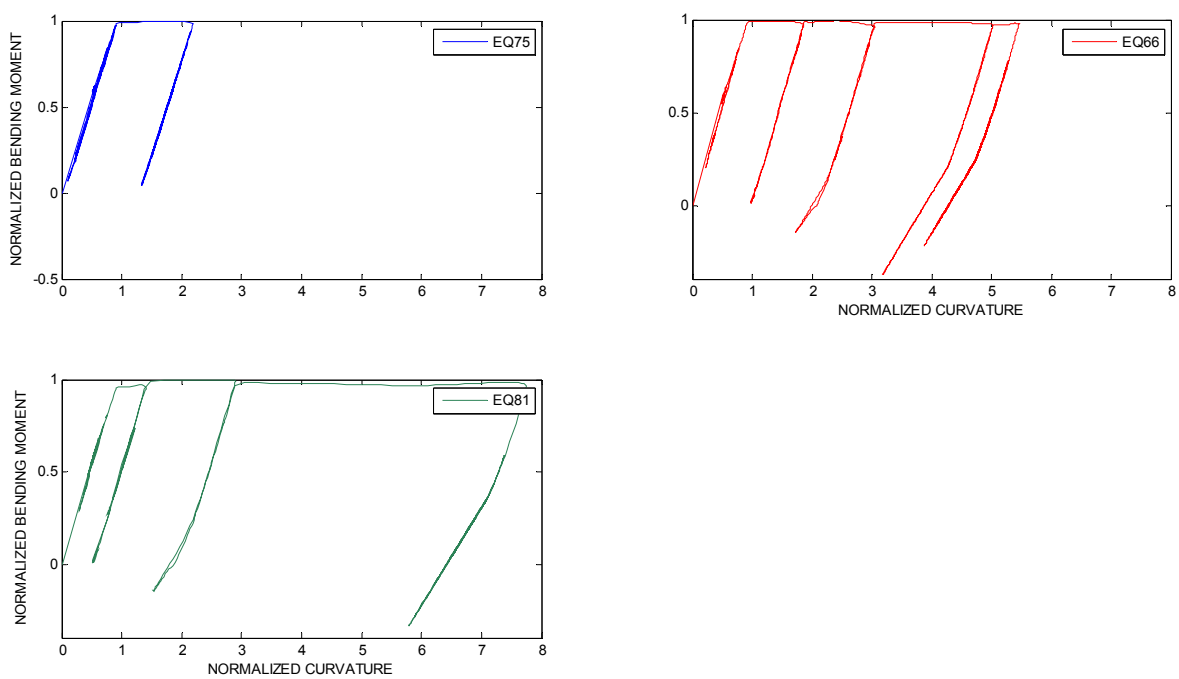

Figure 25: Normalized Beam's Moment-Ductility Demand History.

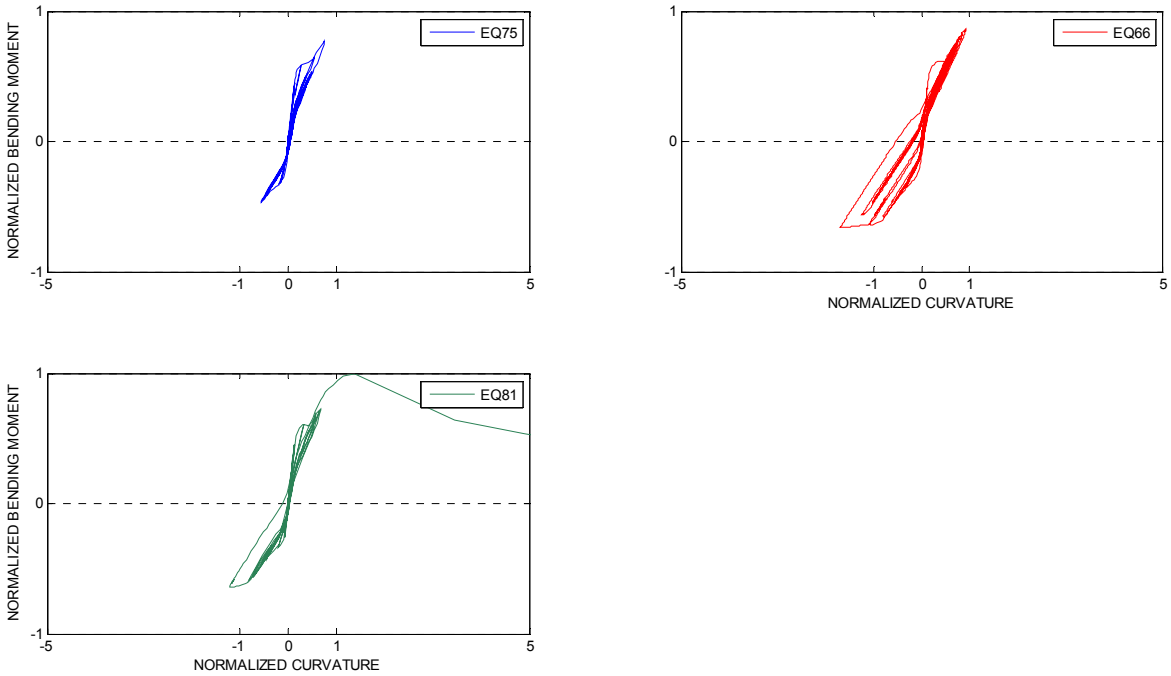

Figure 26: Normalized Wall's Moment-Ductility Demand History.

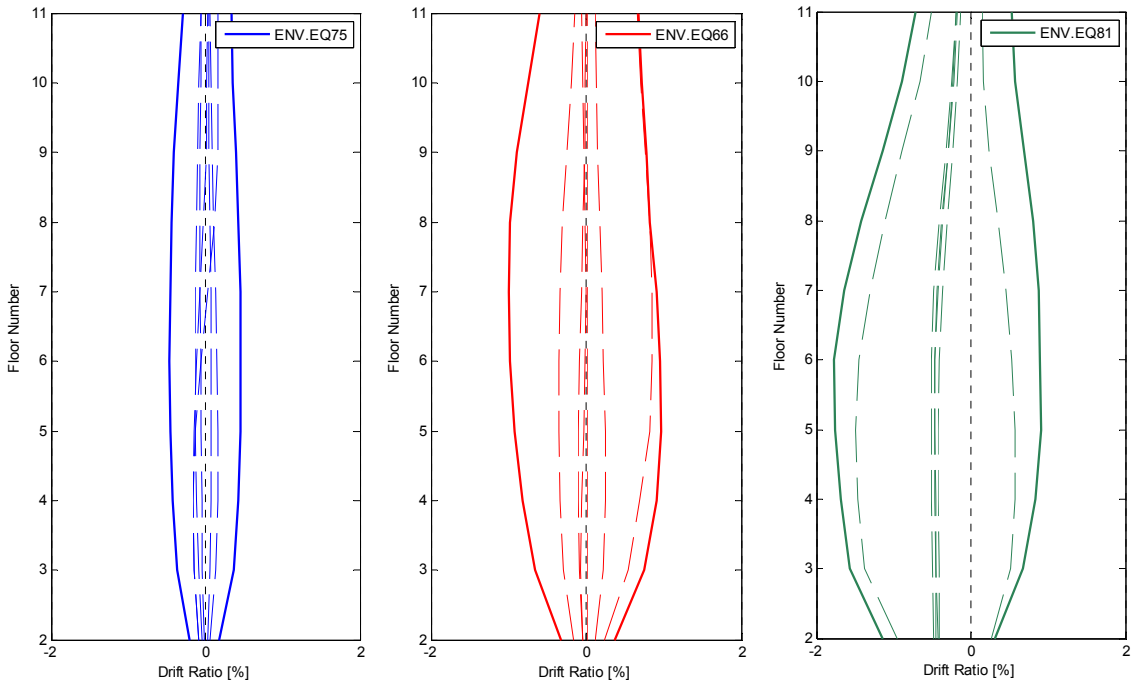

Figure 27: Drift Ratio at each Floor Level.

Figure 28 shows the absolute maximum values for three different responses: a) envelope of the drift ratio per floor; b) envelope of the normalized story shear; c) envelope of the overturning moment at each story. It is shown that the proportionality of the responses is not present in graph b) and c) because of the upper bound limit imposed by the elements moment bending capacities.

These graphs are identical to the ones used for the summary of responses presented in **Section 5.3** for all the different nonlinear dynamic time series analyses performed in this research.

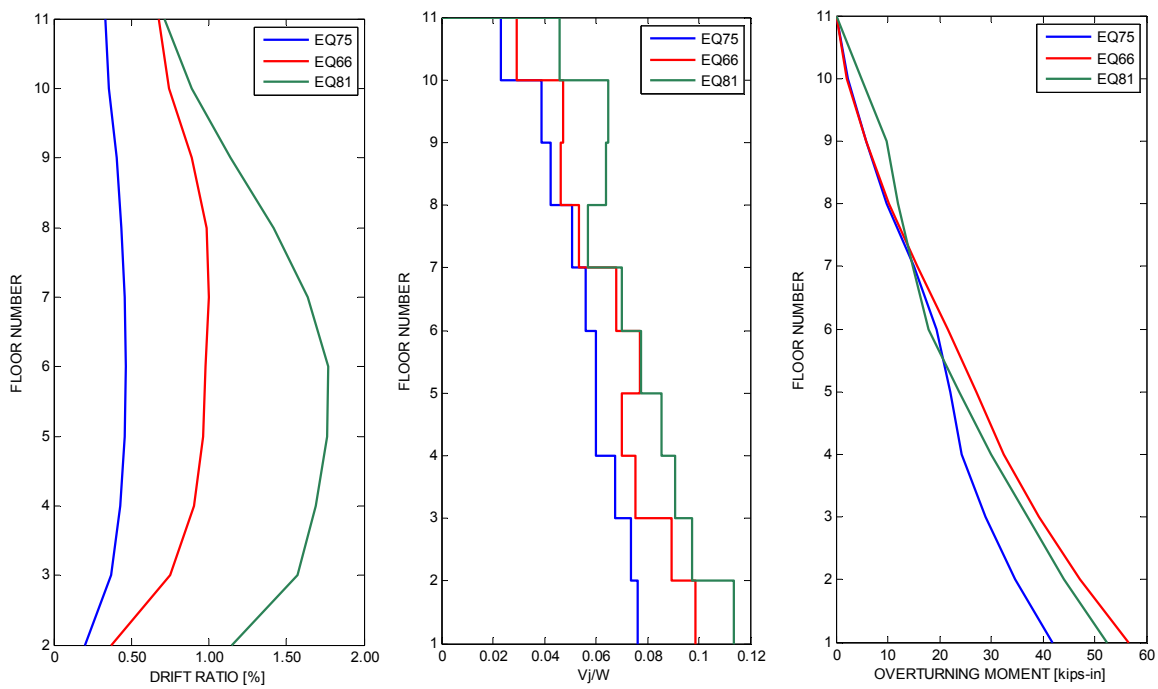

Figure 28: Absolute-valued Envelopes of Different Structural Responses.

5.3 SUMMARY OF RESULTS

This section contains a comparison of the data acquired during the different stages of the research project undertaken. The first part of the summary describes and compares results from the different linear and nonlinear dynamic analyses performed on the structure and also presents data on the nominal strengths of the structural elements. The second part compares results from the nonlinear dynamic analyses with the results gathered from different nonlinear static analyses.

5.3.1 Results from the Nonlinear Dynamic Analyses

In this section the data presented is identifiable with the different colors presented in the graphs. The gray-colored data represents each one of the responses gathered from the 104 ground motions defined in **Section 2.2.** In orange, the median values of those responses (104EQ Median) are presented and in dashed green the corresponding 84th and 95th percentiles. The median of the results gathered from the eight ground motions (8EQ Median) selected in accordance with **Section 2.3** is presented in dashed red. In blue the elastic demand from the modal response analysis is presented and fuchsia represents the nominal strength of the structural elements.

Figures 29 to **32** depict four structural responses at the structural level: maximum acceleration per floor, maximum inter-story drift ratio, maximum story shear and maximum overturning moment.

In **Figure 29** it can be observed that the larger the acceleration demand, the larger the contribution from higher modes to the structural response. The latter is evident from the larger demand present in the middle third of the building if compared to the roof or lower stories demand. The figure also shows a good correspondence between the median results obtained from 104EQ and 8EQ. It can be observed that the variance of the results is larger for events above the median value that are representative of stronger levels of seismic demand.

Figure 30 shows a comparison of the inter-story drift ratios in the building for the different demands used throughout this research project. The drift demand is larger in the middle third of the structure as it is common for typical moment framed structures and is the result of the higher "modes"[10] contribution and the interaction with the wall. The elastic demand is between the 84th and 95th percentile level of the 104 ground motions. The latter is caused by: 1) the fundamental period of the elastic model (used for the design) is larger than the equivalent elastic fundamental period of the nonlinear model ($T_{1elastic_model}$≈2.15s vs $T_{1nonlinear_model}$≈1.80s); this means that the structure is more flexible and will respond with larger displacement to a similar demand[11]; 2) the nonlinear model takes into account the tensile capacity of the reinforced concrete sections to calculate their stiffness and therefore the overall model is less flexible than the elastic model that assumes cracked moment of inertia of the sections as

[10] "Modes" is in quotes because the modal characteristics of a structure are only valid for elastic analyses.

[11] In this statement it is assumed that the good match of the response spectrum used for the elastic design and the median response spectrum of the 104 ground motions represent similar demand characteristics. See **Figure 1**.

recommended by Chapter 10.11 of the ACI 318-05 code. A good correspondence of the demand of 104EQ and 8EQ is evident.

Figure 31 shows the normalized story shears along the height of the building. For this particular figure, the elastic demand with twice the seismic contribution is also presented. The latter is in accord with what is proposed in Chapter 21.12.3[12] of the ACI 318-05 code for intermediate moment frames. It can be observed that the level of seismic demand imposed by the codes through the elastic analysis is below the median values of what is estimated to be the realistic seismic demand (i.e. 104EQ Median > Elastic Analysis +2E). It is apparent that the elastic demand for +1E is as low as the lowest demand imposed by any of the 104 ground motions. The median response due to the selected 8 ground motions matches well with the median of the responses of the 104 ground motions.

Figure 32 depicts the response of the overturning moments per story. Again, the elastic seismic demand is lower than the median response of the 104 ground motions; in fact, it is lower than almost all the responses from the 104 analyses. The 8EQ Median results are almost identical to the 104EQ Median.

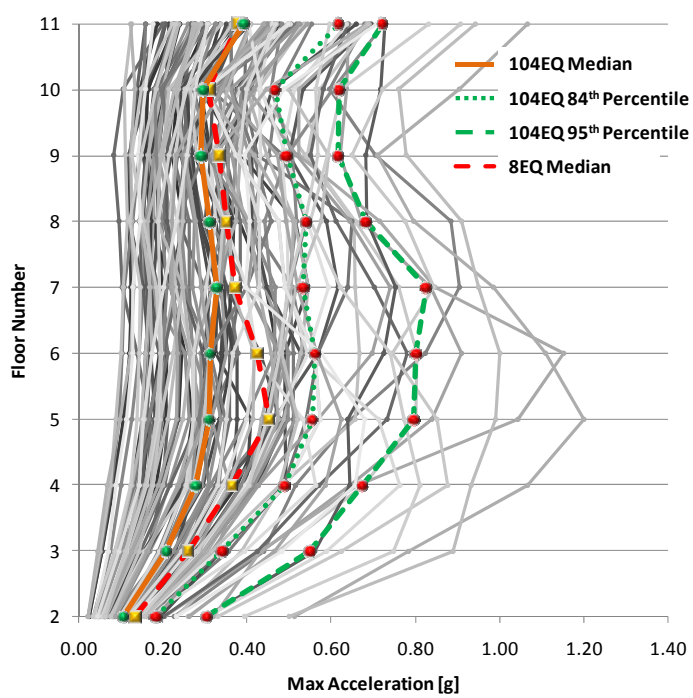

Figure 29: Maximum Acceleration per Floor

[12] "… ϕ ***Vn*** of beams, columns, and two-way slabs resisting earthquake effect, ***E*** , shall not be less than the smaller of (a) and (b):

….

(b) The maximum shear obtained from design load combinations that include ***E*** , with ***E*** assumed to be twice that prescribed by the governing code for earthquake-resistant design."

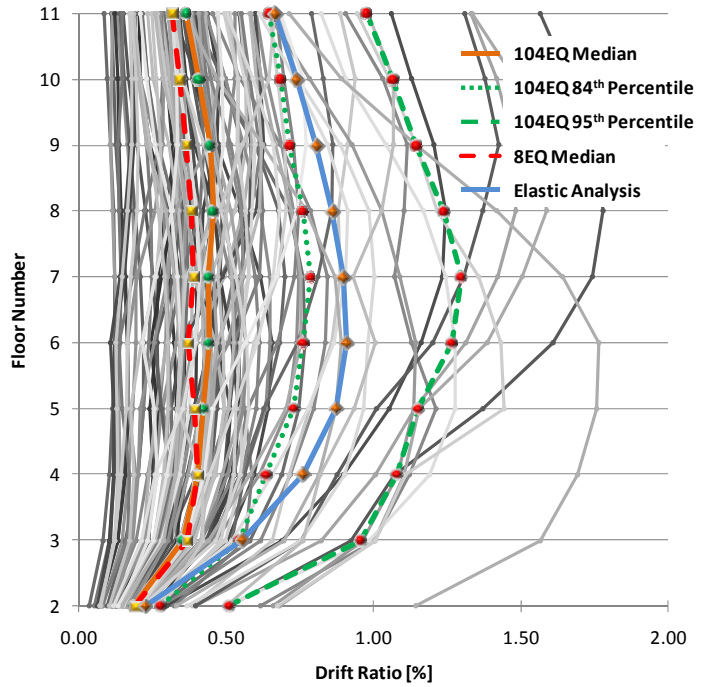

Figure 30: Maximum Drift Ratio per Floor

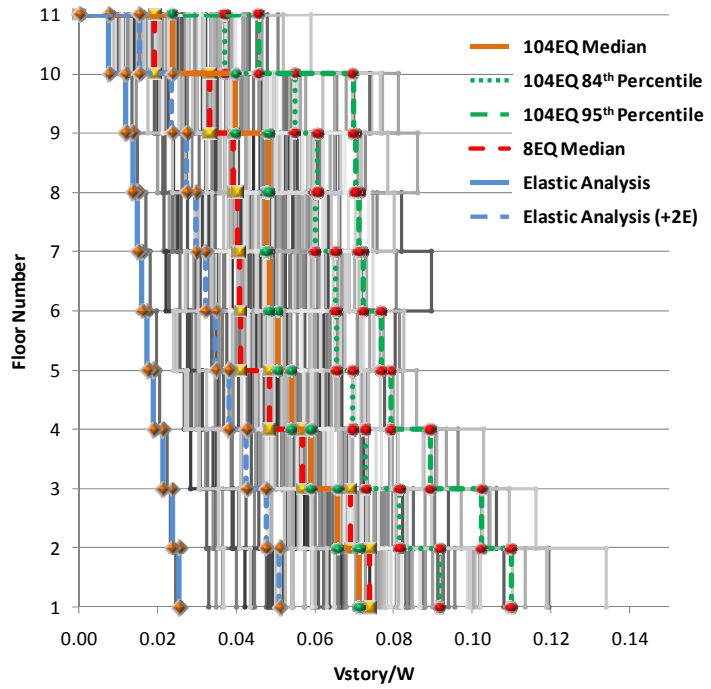

Figure 31: Normalized Maximum Story Shear

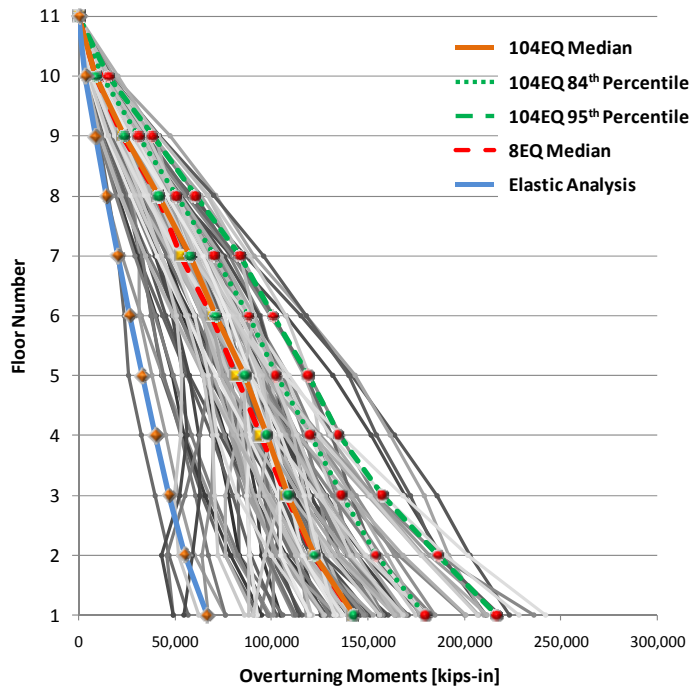

Figure 32: Maximum Overturning Moment per Story

Figures 33 to **37** present the moment bending demand over the columns in the building. Before analyzing the results, it is worth mentioning that the design for their axial-flexure interaction was dominated by minimum requirements for almost all of the sections except for those of the first story in Columns 2 and 3.

The results show that the elastic demand is below the median of the 104 ground motions. Only a few of the time series demanded the columns up to their probable moment capacities (Mpr); the latter was possible thanks to the characteristics of the design nominal strength being much larger than the elastic demand. The results for 8EQ Median and 104EQ Median are almost identical in every floor and every column in the building.

Figures 38 and **39** present the moment bending demand over the ordinary reinforced concrete shear wall. The first of the two figures represent the moment demand that put the flange of the wall in compression. As it is shown in **Appendix C**, for this direction of loading, the wall exhibits a more ductile behavior in its moment curvature relation. It is worth mentioning that the elastic demand for which the first three stories of the wall were designed in this direction (compression in the flange due to bending moment). On the other hand, **Figure 39** shows results for bending moment demand that compress the narrow web of the wall. For this direction of loading, a non-ductile moment-curvature relation is developed by the wall but the nominal strength exhibited is larger.

The results depict that the elastic demand is almost always smaller than 104EQ Median. The only case for which the elastic demand is larger than 104EQ Median case is the one for the bottom of the wall in the direction of loading that compresses the flange of the element (see **Figure 38**). For the upper walls (for which axial-flexural design was governed by minimum requirements) the nominal strength of the wall is surpassed by the demand of the 104 time series in more than 95% and 50% of the cases for the first (flange in compression) and second direction (flange in tension) of loading respectively.

It is important to notice how the elastic demand decreases at the bottom of the first story of the columns. The moment demand pattern is almost constant along the height of the building but decreases in the first story in almost every column because of the higher stiffness of the wall (which "attracts" more elastic demand). It is also shown that the nonlinear analysis does not exhibit that pattern because once the bending moment capacity of the wall is exceeded by the any one of the ground motions, the demand is transferred to the other elements in the story (for this building, these elements are the columns).

For the shear wall, in almost every case, the elastic demand and the median demand of the 104 ground motion exhibit similar distribution shapes along the height of the building. The 104EQ Median value for the bottom of the wall in **Figure 38** exhibits a lower demand with respect to the story above; in this case, the decrease in the demand in the first story can be related to the increase in bending moment demand in the adjacent columns.

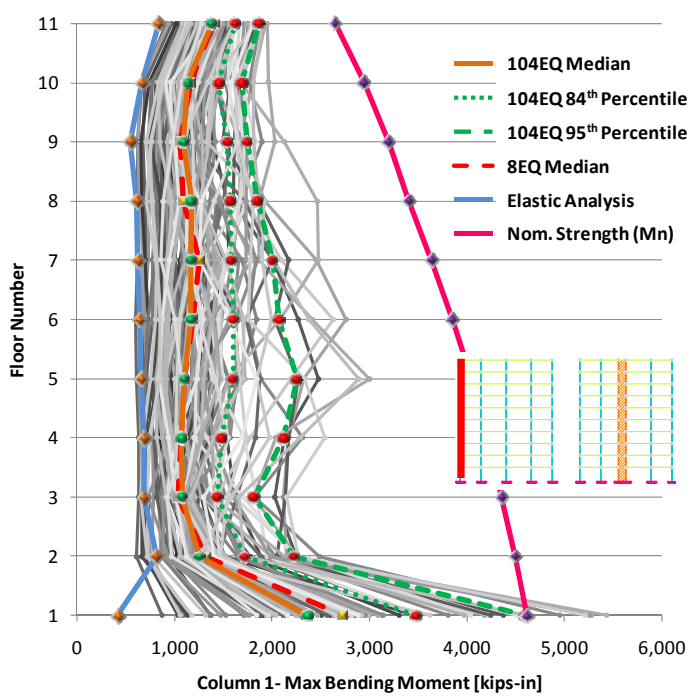

Figure 33: Maximum Bending Moments -Column 1

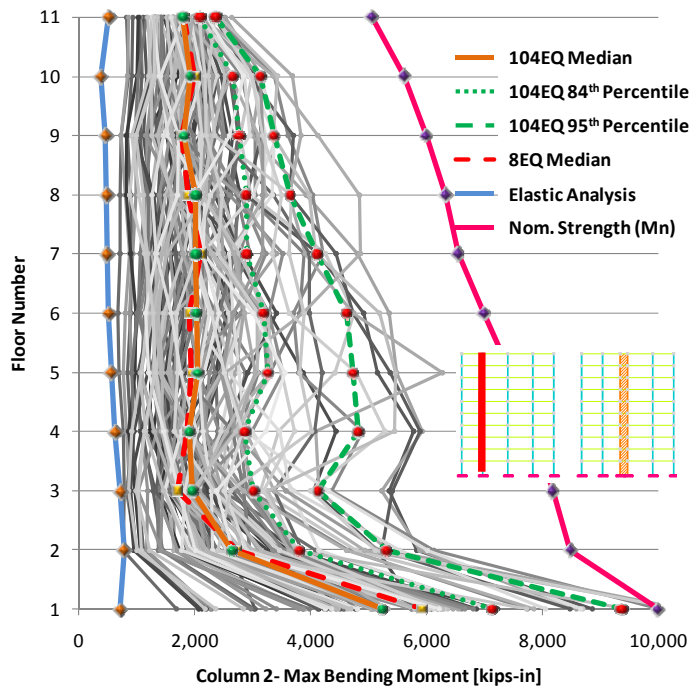

Figure 34: Maximum Bending Moment -Column 2

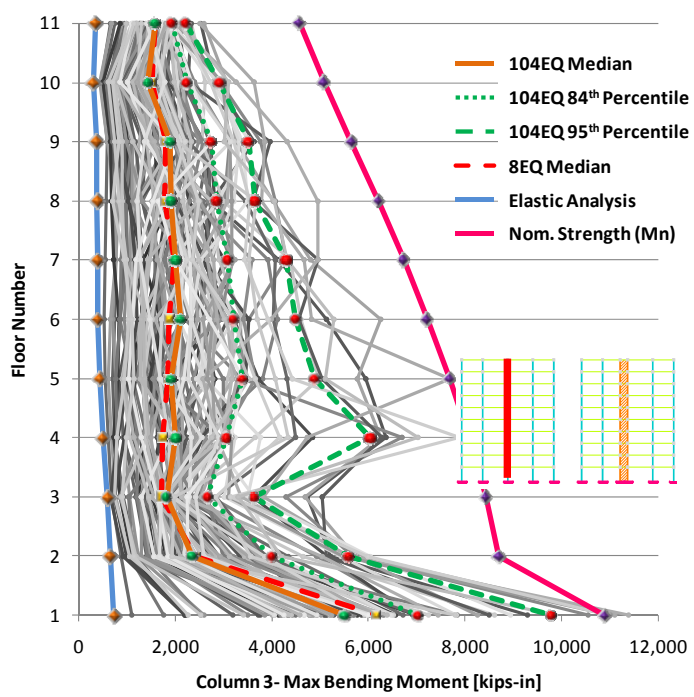

Figure 35: Maximum Bending Moment -Column 3

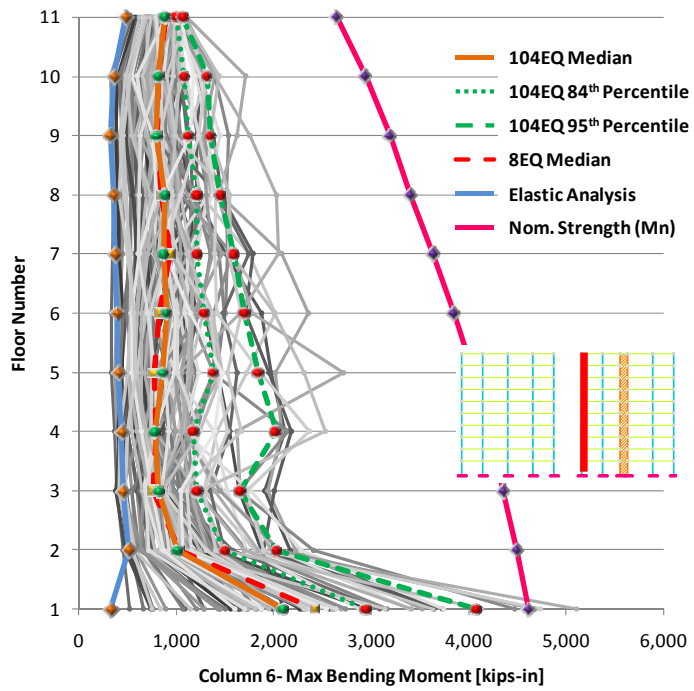

Figure 36: Maximum Bending Moment -Column 6

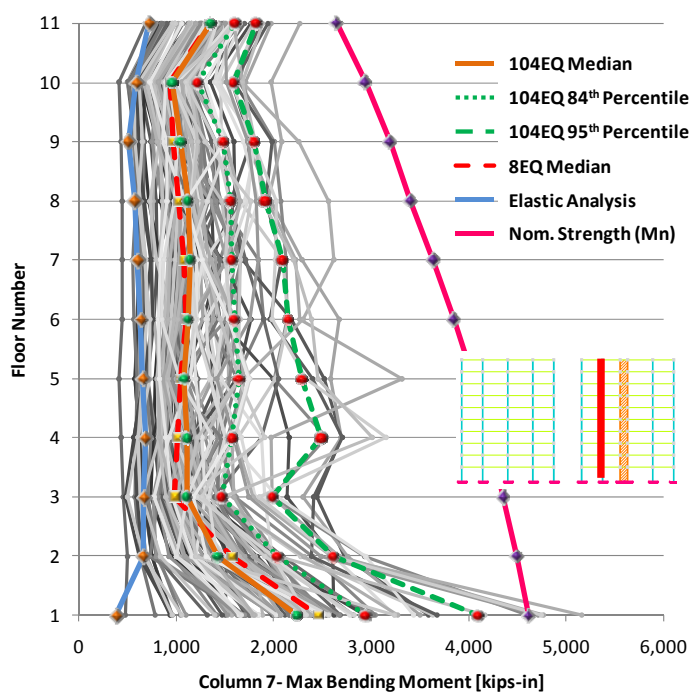

Figure 37: Maximum Bending Moment -Column 7

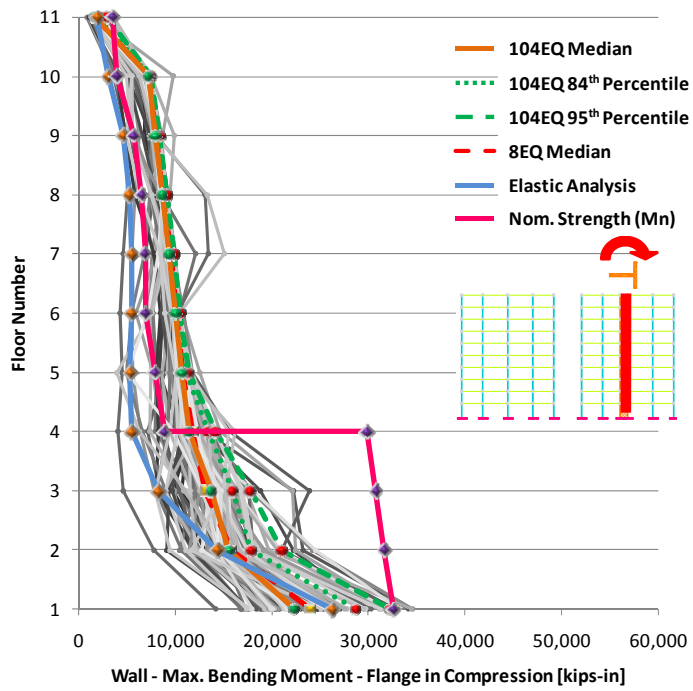

Figure 38: Maximum Bending Moment -Shear Wall. These results are for the bending moments that put the flange of the wall in compression.

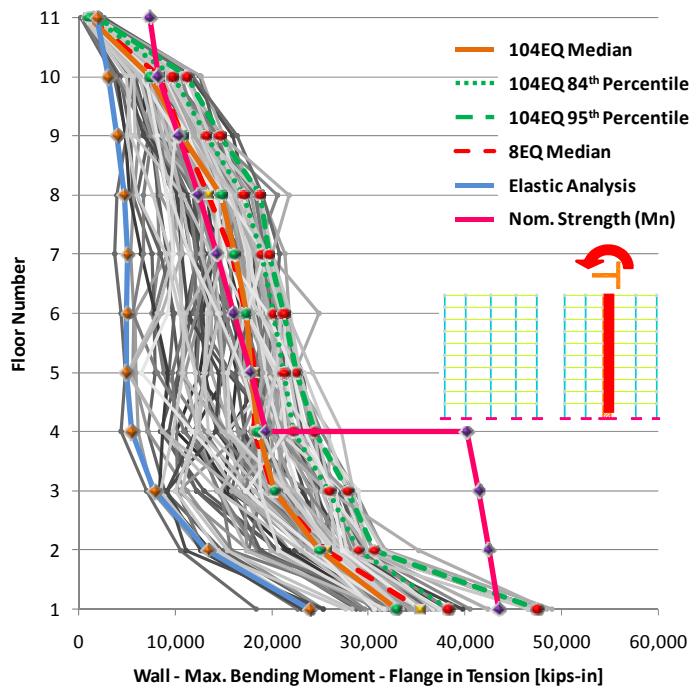

Figure 39: Maximum Bending Moment -Shear Wall. These results are for the bending moments that put the flange of the wall in tension.

Figures 40 to **45** present the shear demand and strength of the columns and the wall.

For the columns, the elastic demand presented is equivalent to the gravity load demand plus twice the seismic load demand as required by Chapter 21.12.3 of the ACI 318-05 code. The nominal shear strength is given by the minimum requirements proposed in Chapter 21.12 of the ACI 318-05 and is larger than the demand in all cases.

The median of the selected 8 time series is very close, in all cases, to the median response of the realistic seismic demand given by the 104 time series. It is interesting to notice that the elastic demand (imposed with twice the seismic load) is almost always smaller than the one from 104EQ Median for the left frame (where the a wall is not present) while it is almost always very close or larger to the median of the 104 ground motions for the columns adjacent to the wall (i.e. Columns 6 and 7).

In all the columns, a decrease in elastic shear demand is exhibited at the first story. Analogous to the case of the bending moment demand, the latter behavior is not shown by the median of the 104 nonlinear analyses performed. Again, the degradation of the stiffness of the shear wall promotes the transfer of shear demand to the columns in the first floor.

The wall's elastic demand does not contain a doubled seismic demand because it is not required by the design codes. It is shown that this elastic demand is smaller than the median of the 104 time series. The shear nominal strengths were calculated to sustain the elastic demand shown but it is apparent that the

realistic demand exceeds the capacity in at least 50% of the cases for almost all the stories. The elastic and nonlinear demand exhibit similar shapes distribution along the height of the structure.

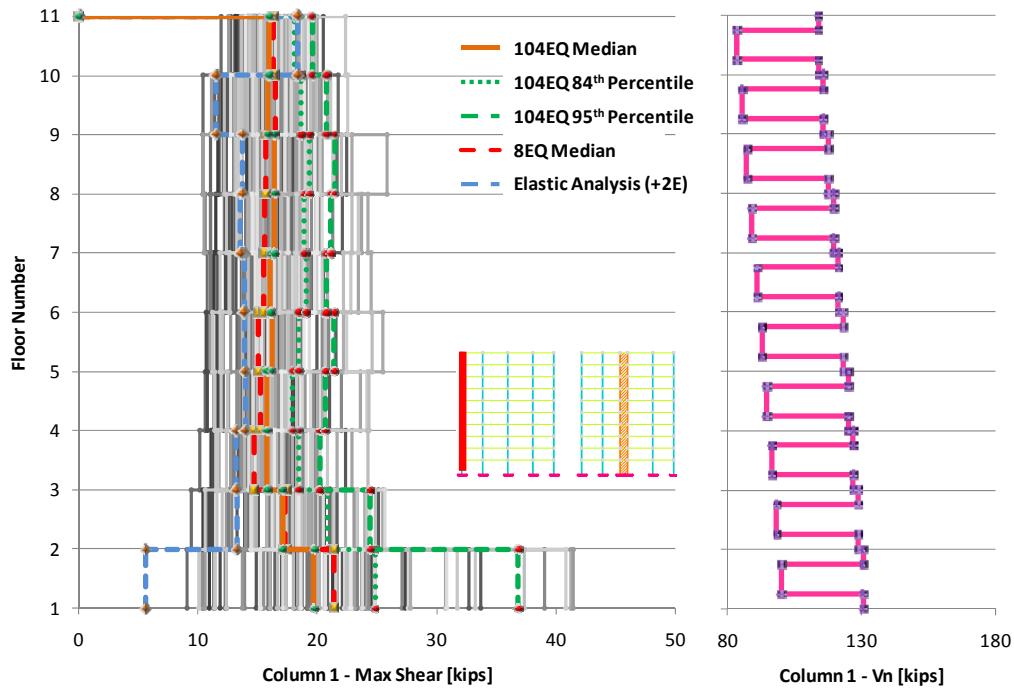

Figure 40: Maximum Shear Demand -Column 1

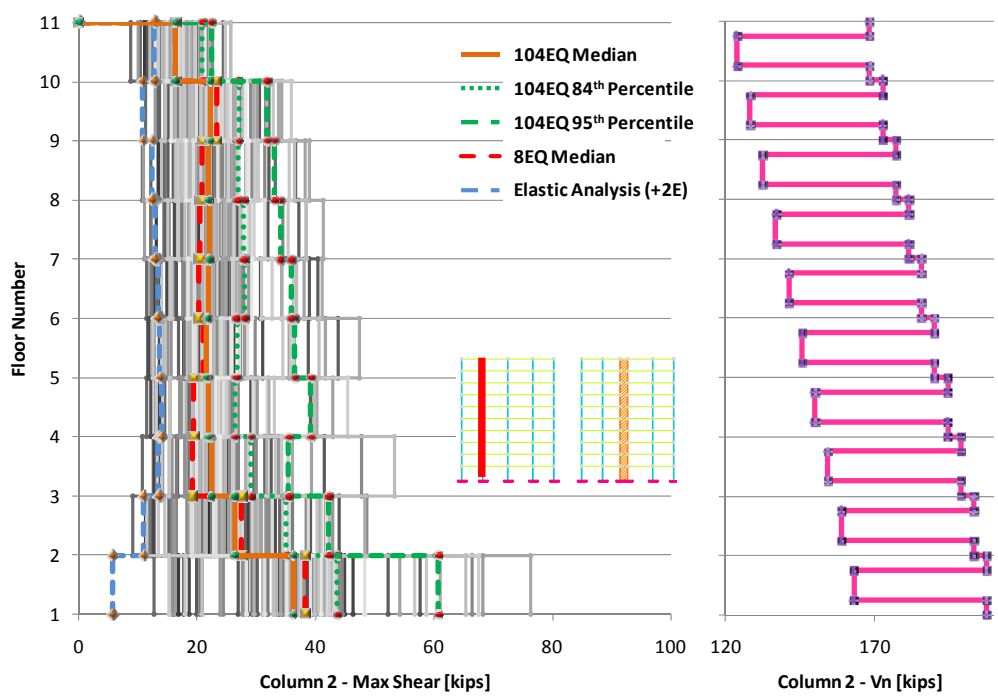

Figure 41: Maximum Shear Demand -Column 2

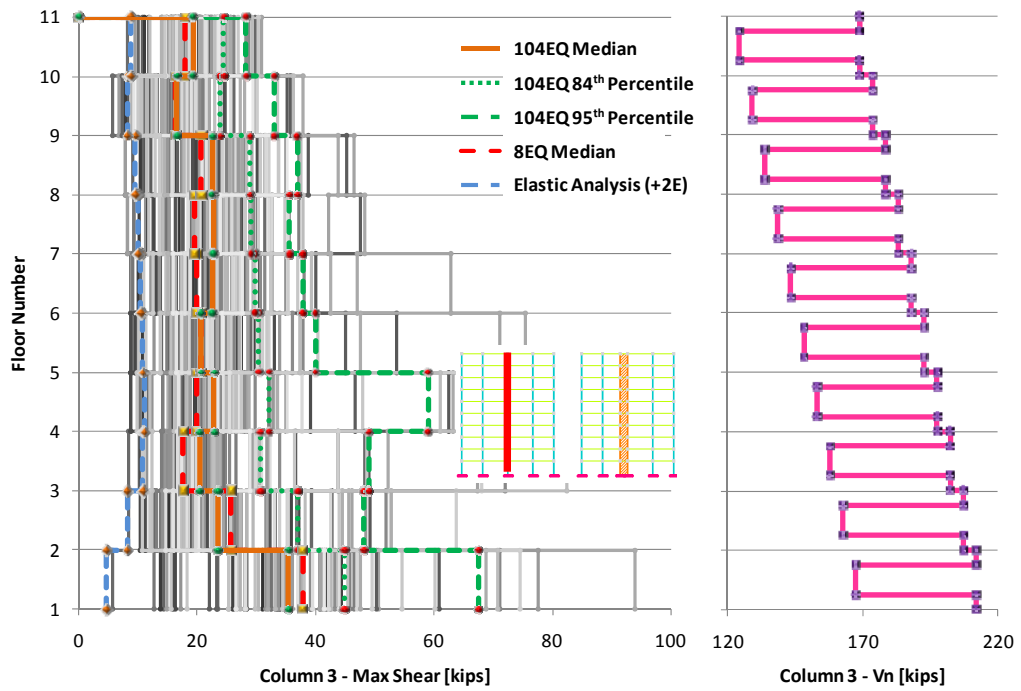

Figure 42: Maximum Shear Demand -Column 3

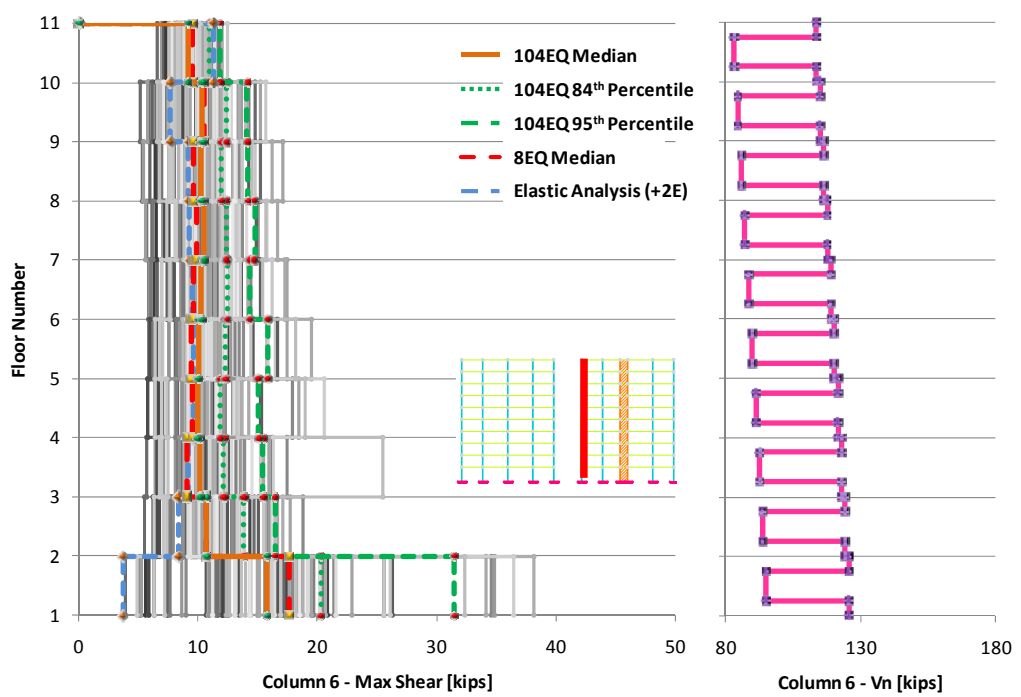

Figure 43: Maximum Shear Demand -Column 6

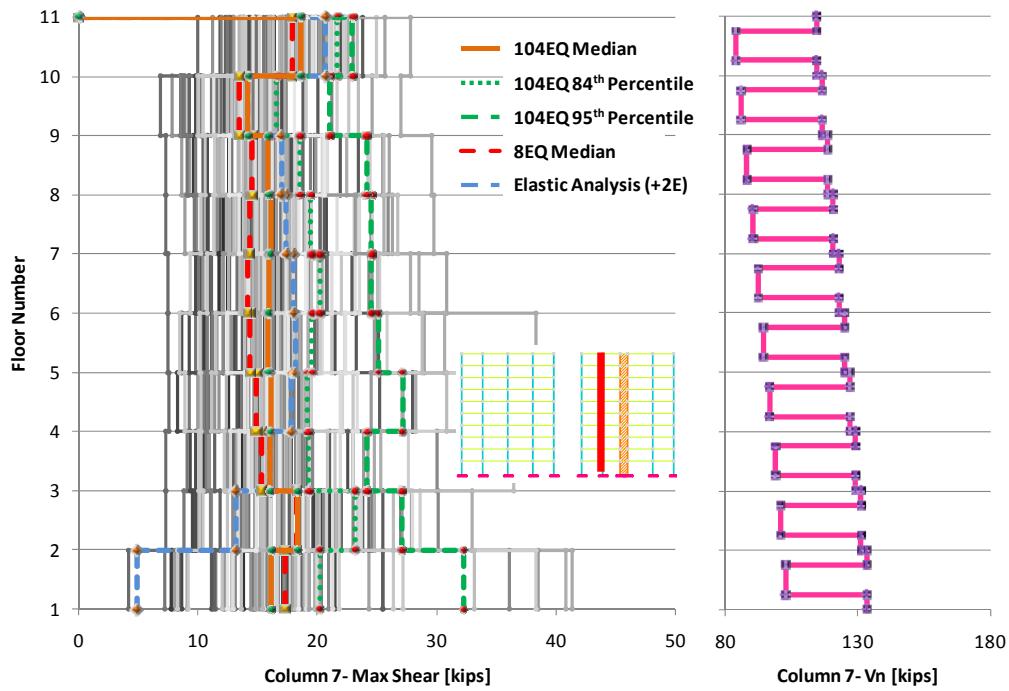

Figure 44: Maximum Shear Demand -Column 7

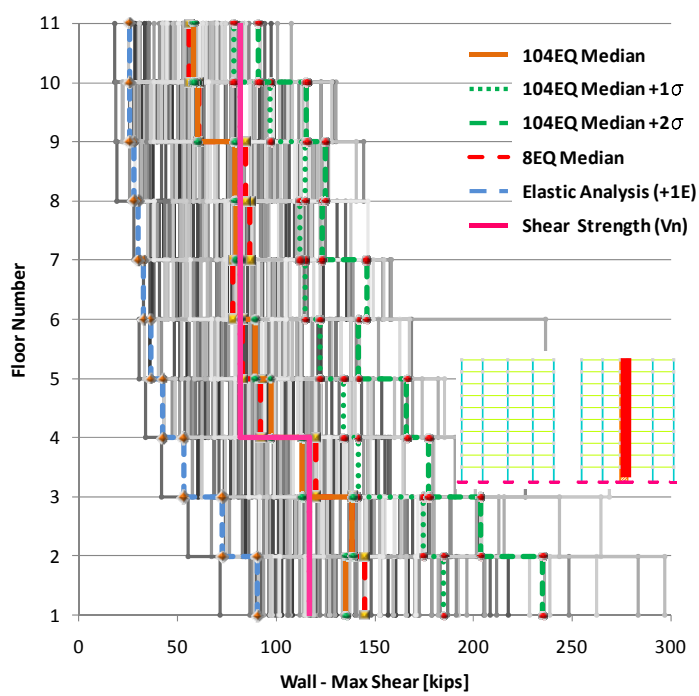

Figure 45: Maximum Shear Demand -Shear Wall

Figures 46 and **47** contain histograms of the ductility demand of the bottom (IP-1) and top (IP-5) sections of the wall at every story. In the graphs, negative values are for demands that compress the wall's flange; as explained before, for this direction of the loading, the wall's section exhibits a ductile moment-curvature relation; for the latter case, none of the 104 ground motions exceeded the ductility capacity of the wall. For the opposite case of loading, the limiting value of the ductility demand is $\mu_{max} = 5$ because of the non-ductile behavior exhibited by the moment-curvature relation. In this case less than 6% the 104 time series demanded the wall to ductility values larger than its capacity.

Figures 48 and **49** contain histograms that represent the ductility demand on the columns and beams respectively. The graphs show the frequency of ductility demand per floor for the most demanded column and/or beam. The levels of demand in these elements are low and within the element's capacity.

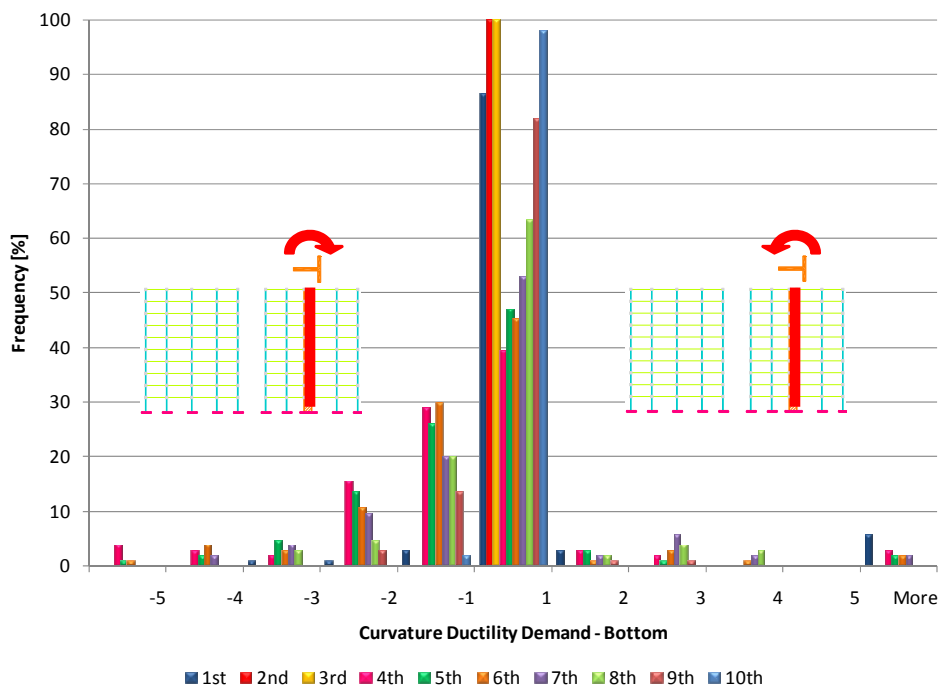

Figure 46: Wall's Ductility Demand Histogram for the 104 Ground Motions - Lower Section.

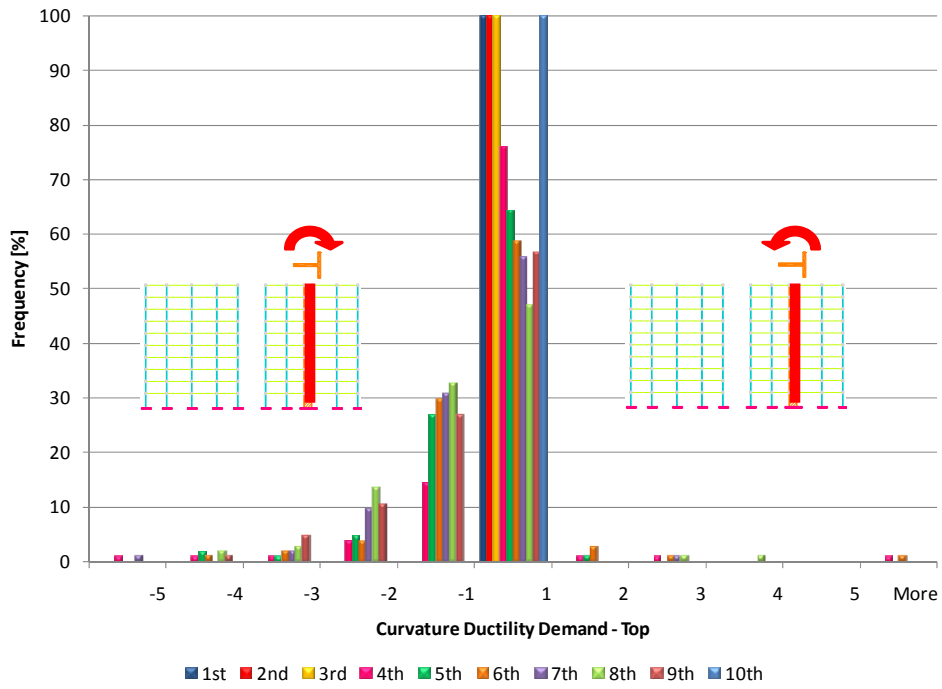

Figure 47: Wall's Ductility Demand Histogram for the 104 Ground Motions - Upper Section.

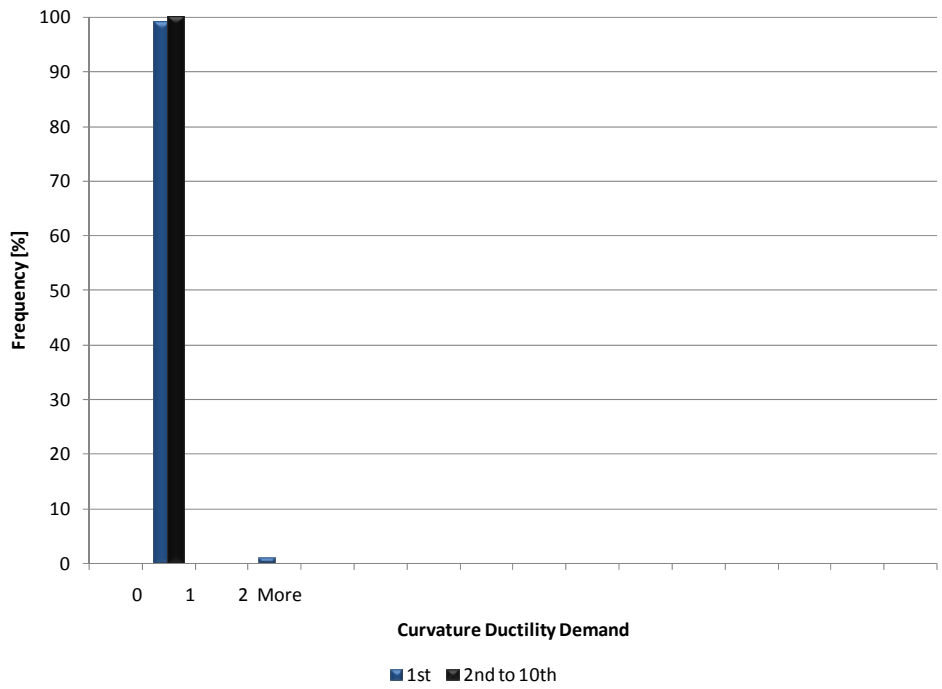

Figure 48: Column's Ductility Demand Histogram for the 104 Ground Motions.

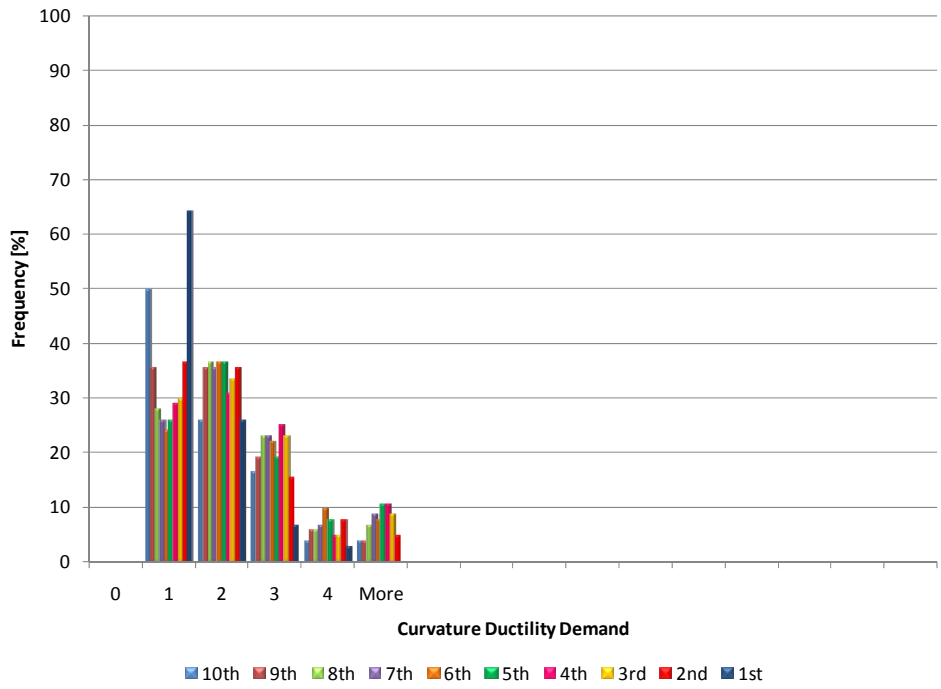

Figure 49: Beam's Ductility Demand Histogram for the 104 Ground Motions.

5.3.2 Results from the Nonlinear Static Analyses

Pushover curves of the structure were developed for the two horizontal directions. As shown in **Figure 50**, two types of loads were used for this stage of the research: 1) rectangular loading pattern with constant distribution of the load at every floor and 2) first mode shape loading pattern with concentrated loads (at every floor) that are proportional to the elastic first mode shape of the structure.

The data shown in **Figures 51** to **60** was obtained at three different levels of roof displacement: 1)$\triangle_{roof_target1}$=0.35% corresponds to a level of displacement demand that matches the median displacement response of the roof to the 104 ground motions (104EQ Median); 2)$\triangle_{roof_target2}$=1.00% corresponds to a level that is equivalent to the target drift ratio chosen for elastic analysis and design of the structure;3)$\triangle_{roof_target1}$=2.50% corresponds to a level that is equal to the maximum allowable drift ratio according to Table 12.12-1 of the ASCE/SEI 7-05.

Figure 50 shows the four pushover curves developed for this section. It can be seen that the maximum roof displacement target corresponds to a global drift ratio of 2.5%. Even though the pushover curves reach different values of maximum base shear, they have similar shapes with apparent jumps due to strength degradation of the structural elements. This degradation is generated by the loss of strength of the sections of the wall when the narrow extreme of the web is compress to large strain values.

It is worth mentioning that the drift ratios at which the P-$\triangle$ effect triggers the softening (relative negative slope of the pushover curves) of the structure, varies for the positive and the negative direction of loading. For the first direction of loading, negative structural stiffness can be observed between 1.30% and 1.80% drifts. For the negative direction of loading, the negative slopes in the force-displacement relations shown are observed after the abrupt loss of strength at values of drift ratio between 0.80% and 1.00%

Figures 51 to **53** show a comparison of the maximum structural responses gathered for the three levels of roof displacement. The median, 84th percentile and 95th percentile values of the response to the 104 ground motion selected in **Section 2.2** are also depicted.

As it is expected, the drift ratios shown in **Figure 51** are proportional to the displacement demands imposed to the roof level. Apparent is the good correlations between the values obtained for $\triangle_{roof_target1}$=0.35% and the median from the 104 time series analyses. From the four distributions corresponding to $\triangle_{roof_target2}$=1.00% and $\triangle_{roof_target3}$=2.50% it can be observed that the rectangular loading pattern demand the lower middle of the structure more than the 1st mode-shape loading pattern. The demand for $\triangle_{roof_target2}$=1.00% is at the level of 95th percentile of the 104 analyses. The drift demand for $\triangle_{roof_target3}$=2.50% is much larger than almost any one of the 104 series analyzed.

Figure 52 contains the distribution of the maximum shear demand per story. It can be observed that the curves corresponding to rectangular loading pattern give an upper bound limit for the base shear de-

mand. For the lower levels, the shear demand for $\Delta_{roof_target2}$=1.00% and $\Delta_{roof_target3}$=2.50% are close to the level of 84th percentile of 104EQ; the median value of 104EQ is closer to the demand for $\Delta_{roof_target1}$=0.35%. For the upper levels, the demands for all the pushover curves are smaller than the median of the 104 analyses. Higher "mode" contributions in the dynamic analysis are the cause for the disparity in the behavior described before. None of the demand from the static analysis is at the level of the 84th percentile of the 104 ground motions analyses.

The overturning moment distribution is presented in **Figure 53**. It can be seen how the upper bound for the distribution is reached at roof displacements levels larger than the imposed by $\Delta_{roof_target2}$=1.00%; the latter is evident from the overlapping of the graphs for $\Delta_{roof_target2}$ and $\Delta_{roof_target3}$. The overturning moment distribution for the statics cases do not seem to correlate adequately to any of the dynamic ones. It is believed again that the contribution of higher "modes" is the cause for the differences exhibited.

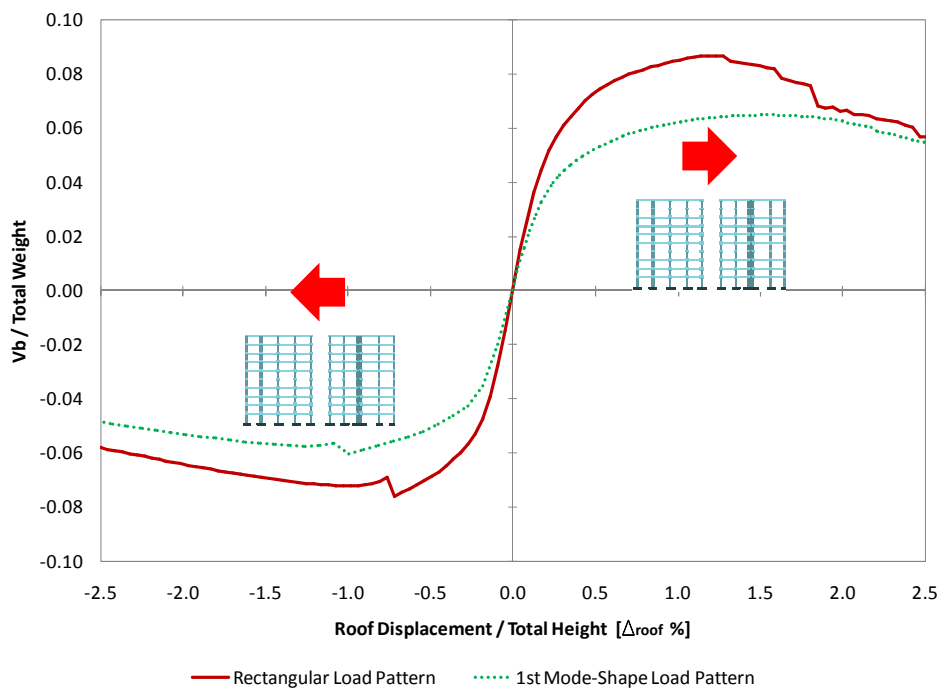

Figure 50: Pushover Curves.

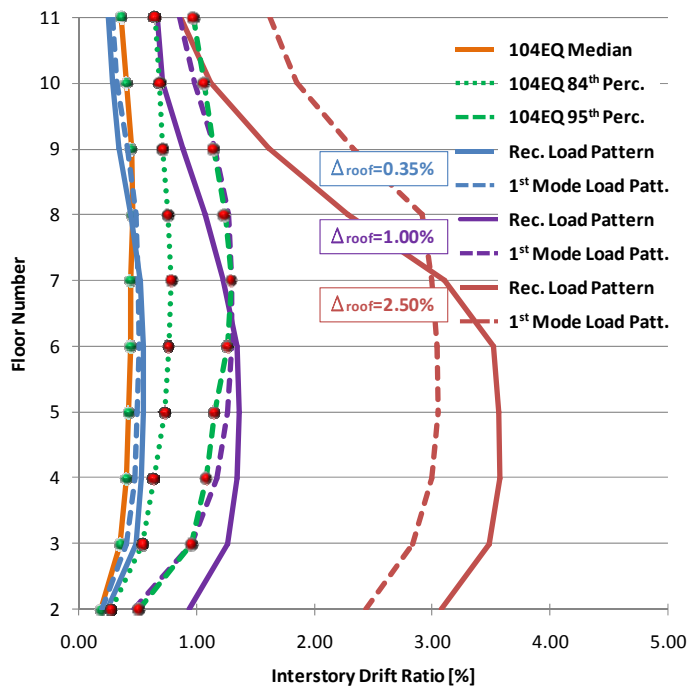

Figure 51: Comparison of the Distribution of the Inter-story Drift Ratios for the Nonlinear Static and Dynamic Analyses.

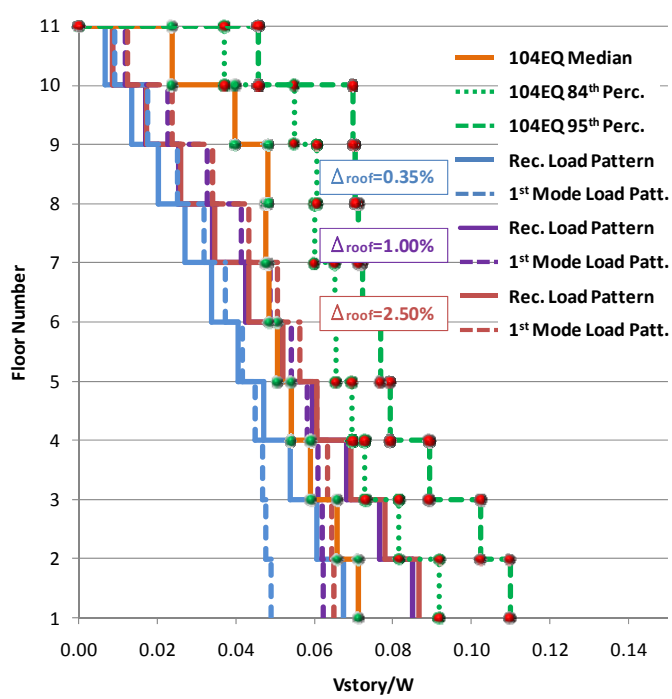

Figure 52: Comparison of the Distribution of the Normalized Shear per Story for the Nonlinear Static and Dynamic Analyses.

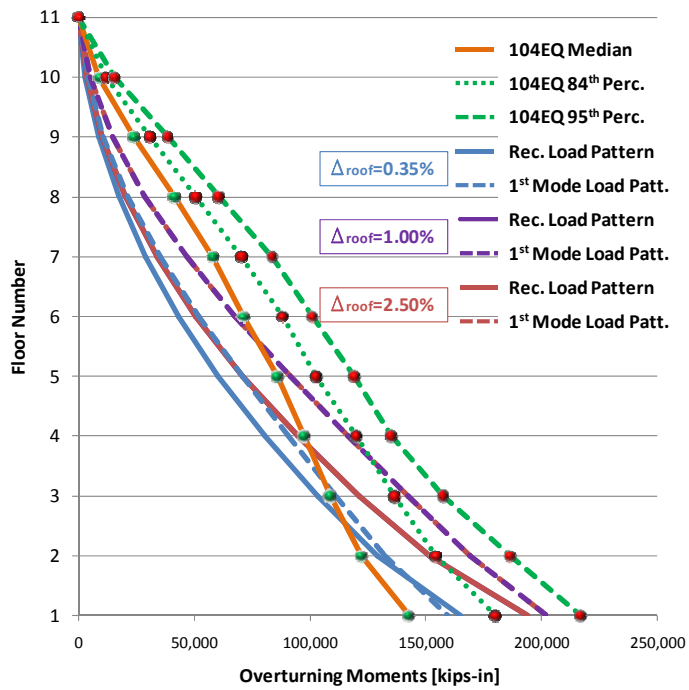

Figure 53: Comparison of the Distribution of the Overturning Moments for the Nonlinear Static and Dynamic Analyses.

Figures 54 to **57** show maximum values of bending moment and shear demands calculated for two representative columns and the shear wall. A comparison of the results gathered from the different pushover analyses and the median, 84th percentile and 95th percentile values of the response to the 104 dynamics analysis is drawn in each figure.

In the graphs for the columns, it can be seen how the different levels of roof displacement promote extra bending moment demand along the height of the building. The median of 104EQ is, to some extent, similar to the static demand for $\triangle_{roof_target1}$=0.35%. The nominal strength of the columns is only exceeded at the bottom of the first story by $\triangle_{roof_target}$≥1.00% and for Column 3 (the most demanded one in all the analyses performed) it is exceeded at higher levels by the $\triangle_{roof_target3}$≥2.50%. It is interesting to describe that the demand at the 4th floor stays almost unchanged for the three levels of static demand with the rectangular loading pattern. For the 1st mode-shape loading pattern, the same behavior is observed at the 5th floor. Around these levels is where the moment demand in the shear wall presents an inflection point of zero bending moment.

As described before, the wall exhibits a double curvature moment demand along its height. The behavior shown for the wall is exceeding the nominal strength in almost every floor for all the loading patterns and directions. The upper bound of the maximum demand shown for all the analyses performed is given by the bending moment capacities of the wall's sections. Even the lowest roof displacement demand pushes the wall to its strength limit in the upper stories. The fact that a plastic hinge is formed at the bottom of the first story is the cause why the wall is demanded under its maximum capacity in the second and the third story.

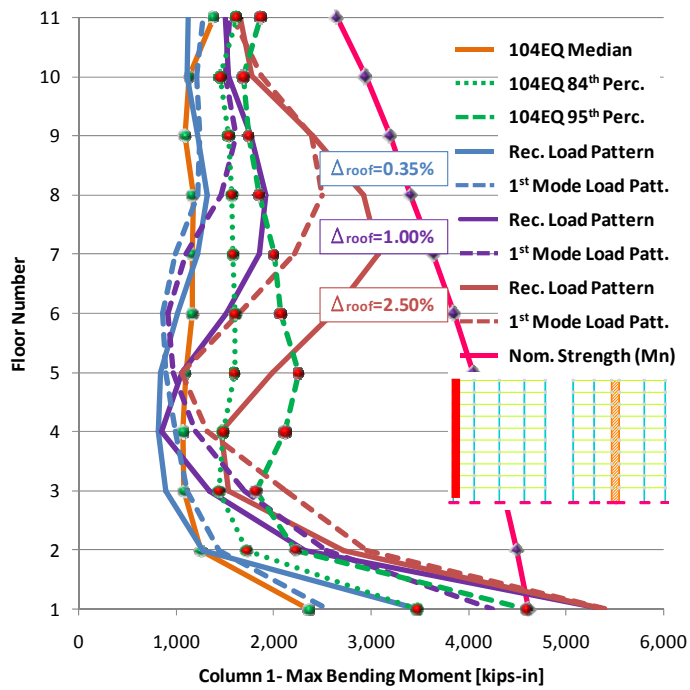

Figure 54: Comparison of the Distribution of Bending Moment Demand on Column 1 for the Nonlinear Static and Dynamic Analyses.

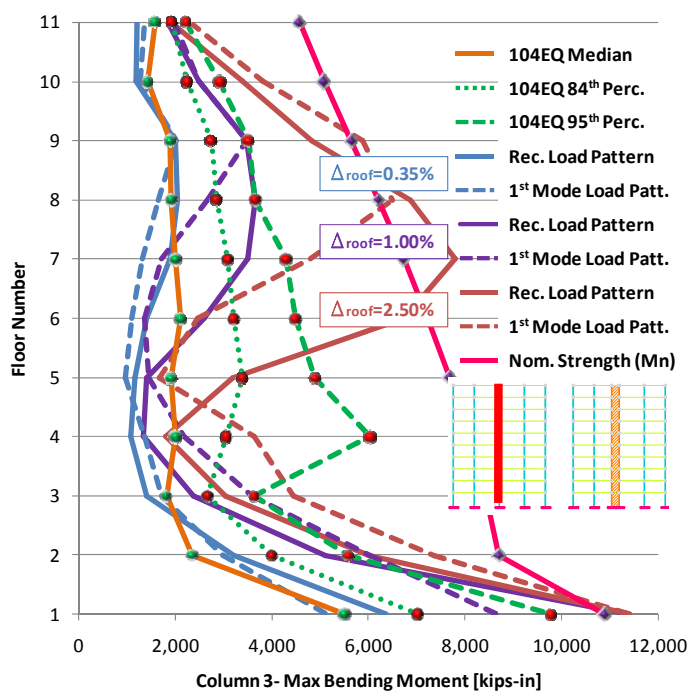

Figure 55: Comparison of the Distribution of Bending Moment Demand on Column 3 for the Nonlinear Static and Dynamic Analyses.

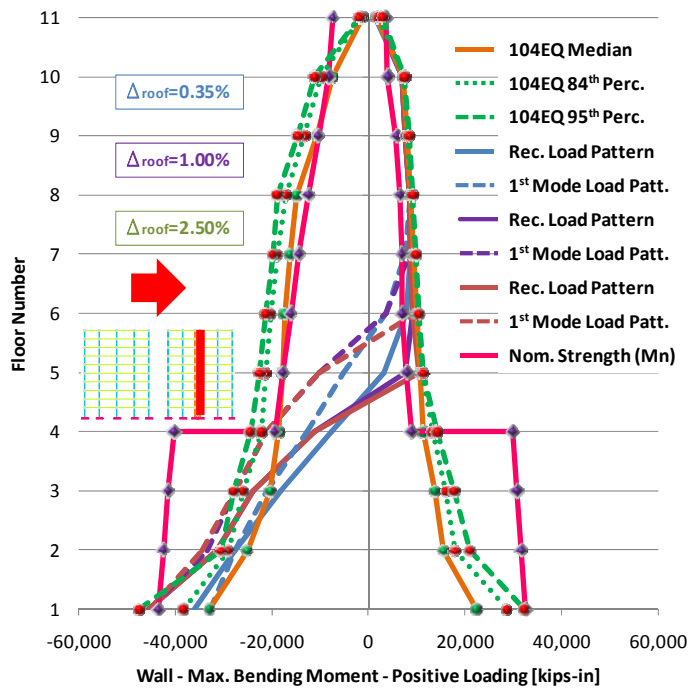

Figure 56: Comparison of the Distribution of Bending Moment Demand (Positive Direction of the Loading) on the Wall for the Nonlinear Static and Dynamic Analyses.

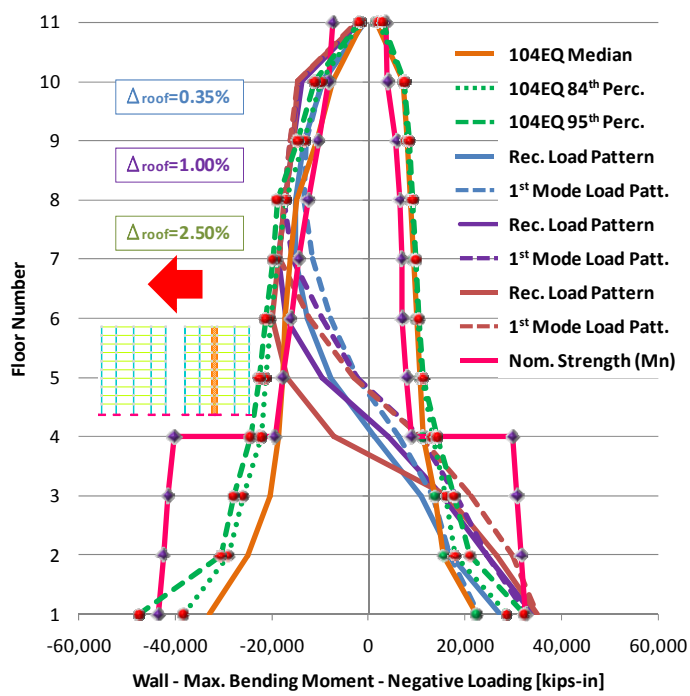

Figure 57: Comparison of the Distribution of Bending Moment Demand (Negative Direction of the Loading) on the Wall for the Nonlinear Static and Dynamic Analyses.

Figures 58 to **60** show analogous results to the ones described above for the case of shear demand. It can be seen in **Figure 58** that the variation of the shear distribution seems almost constant for the upper levels of Column 1 with every loading pattern. A similar behavior is exhibited by the median of 104EQ. The shear demand in the first story is much larger than the one at other stories and is the response of the transfer of demand once the bending moment capacity of the wall is reached.

In **Figure 59** a transition of the demand (to the upper levels) is observed for $\Delta_{roof_target3} \geq 2.50\%$. The same extra demand evidenced by Column 1 is present in Column 3 at the first story. For this column, higher levels of roof displacement promote an increment in the shear demand that is in accord to the one exhibited for bending moment in the upper levels.

The shear demand in the wall is presented in **Figure 60**. It is apparent how at the first story almost for all the loading patterns, the shear demand experiences a reduction with respect to stories that are immediately above. The formation of a hinge due to excess of demand at the bottom the wall is the cause for the latter behavior.

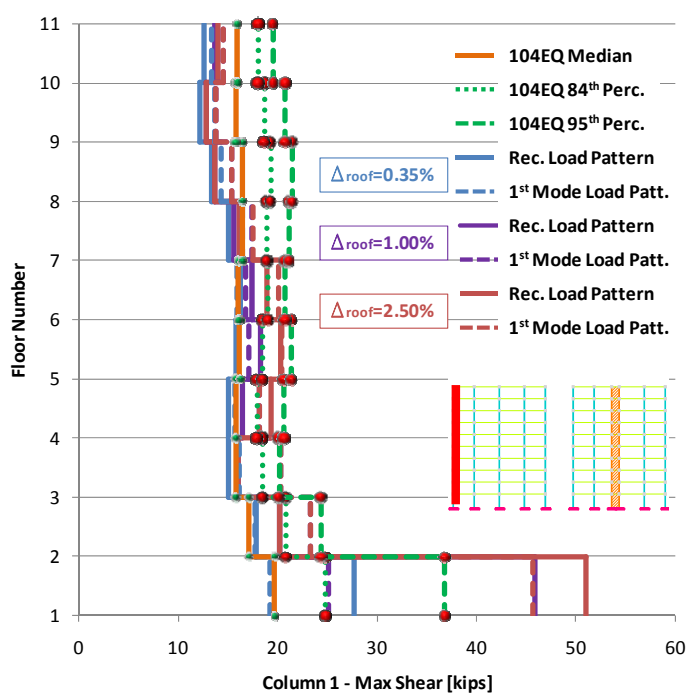

Figure 58: Comparison of the Shear Demand on Column 1 for the Nonlinear Static and Dynamic Analyses.

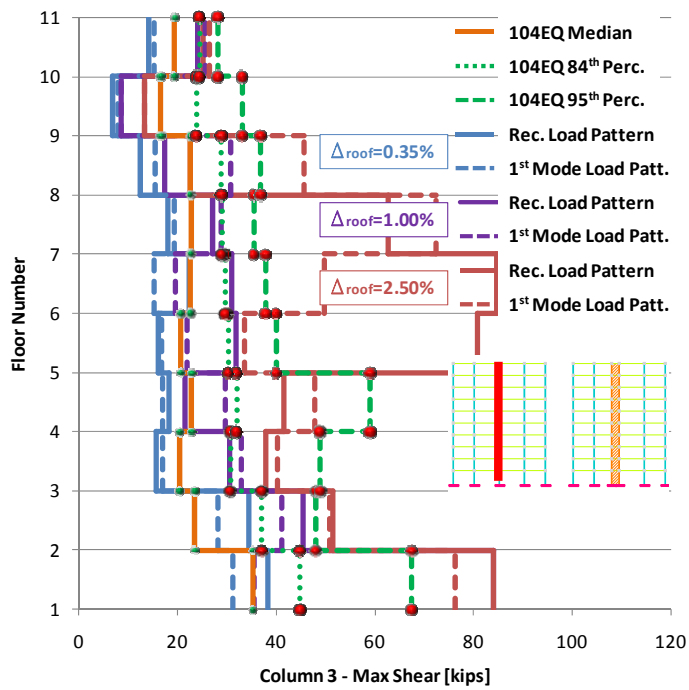

Figure 59: Comparison of the Shear Demand on Column 3 for the Nonlinear Static and Dynamic Analyses.

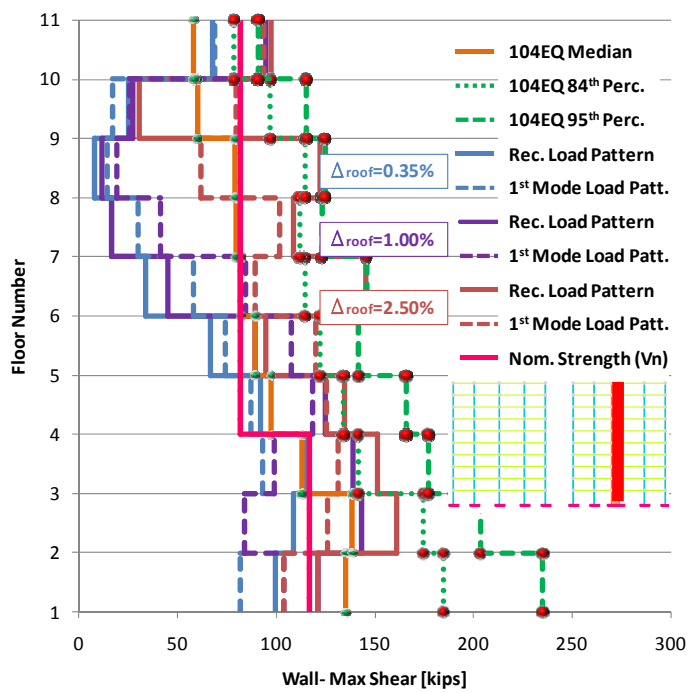

Figure 60: Comparison of the Sheat Demand on the Wall for the Nonlinear Static and Dynamic Analyses.

Results shown in **Figures 61** and **62** intend to give an idea of the behavior of the non ductile shear wall and compare its result with the one of a the highly demanded ductile Column 3. The stories shown were selected because at those locations, the shear wall behaved nonlinearly.

From **Figure 61** it is apparent how some of the upper walls ductility demand curve jumps abruptly even for lower values of roof drifts ($\triangle_{roof}$ <0.25%). The fact that design of the lower sections of the wall (1st, 2nd and 3rd stories) contains a boundary element, is the reason why the 1st story wall exhibits a more ductile behavior once the yielding curvature is reached.

The case of the Column 3 shown in **Figure 62** is less dramatic. Once the yielding curvature is reached the ductility demand for curvature grows steadily without abrupt changes. It is worth mentioning that the ductility demand for the column becomes larger than the yielding value at a roof drift that generates the abrupt jump in ductility demand of the first story wall shown in **Figure 61**.

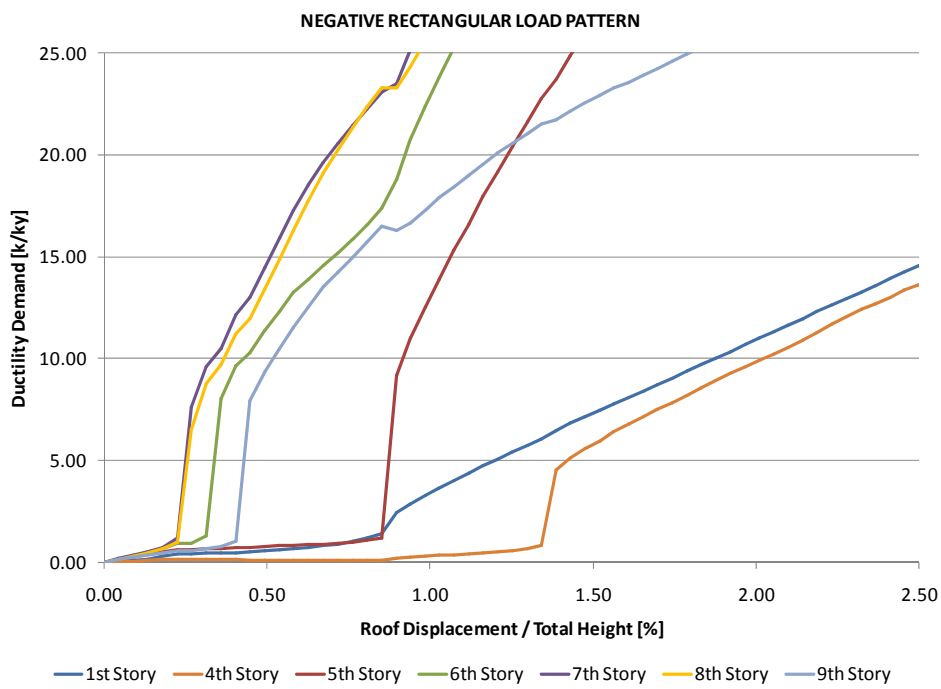

Figure 61: Curvature Ductility Demand versus Normalized Roof Displacement under Rectangular Load Pattern - Shear Wall.

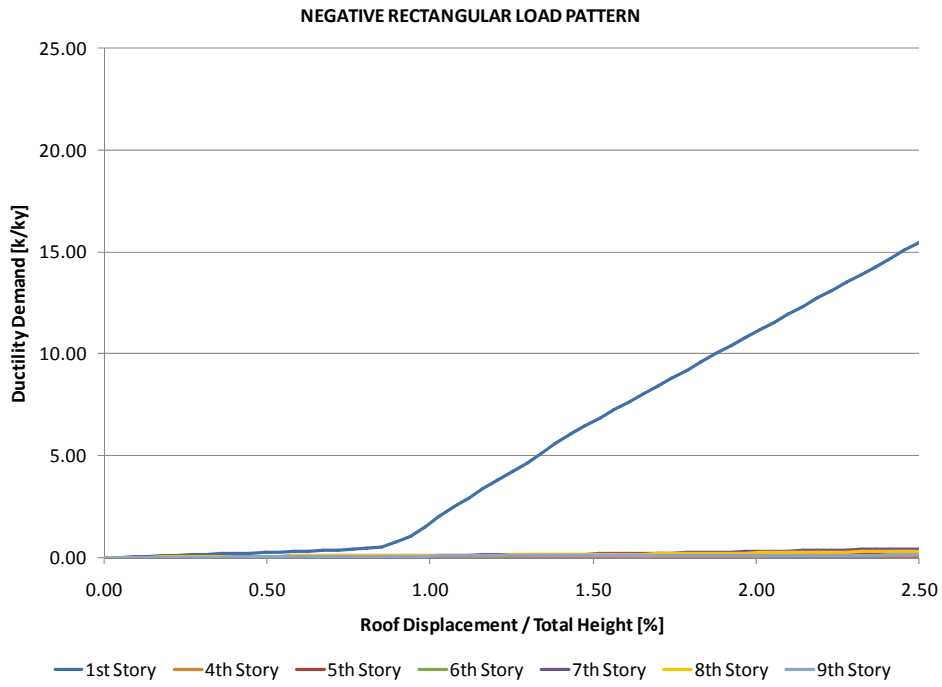

Figure 62: Curvature Ductility Demand versus Normalized Roof Displacement under Rectangular Load Pattern - Column 3.

5.4 IMPLICATIONS OF RESULTS

In this section some conclusions are drawn with respect to various aspects of what is considered to be adequate by the building codes for the analysis and design of an intermediate reinforced concrete moment framed structure. The series of nonlinear dynamic analyses performed throughout this research project allowed to gather information of what is considered a more realistic behavior of the structure under a seismic hazard level comparable to the one proposed by the codes but defined in a more rational way.

5.4.1 Elastic Demand versus Realistic Results

It has been shown throughout **Section 5.3.1** that the elastic seismic demand that correspond to a design spectrum reduced by a Response Modification Coefficient R=5.0 are too small to even match the median demand imposed by the realistic scenario of seismic hazard level. Not even the provision proposed by the ACI 318-05 code to calculate the shear demand using double the design seismic load (2E) seems to be large enough to match median levels of realistic seismic demand due to the mismatch in the assumed reduction of strength factor of one fifth the elastic capacity of the structure.

The fact that the median demand in the structural elements is larger than the one proposed by the codes trough and elastic modal dynamic analysis is caused by two main factors: 1) the equivalent elastic period of the nonlinear model is shorter than the one used in the elastic analysis and design ($T_{1nonlinear_model}$≈1.80s versus $T_{1linear_model}$=2.15s); 2) the ratio between the elastic demand and the realistic yielding strength of the structure is not as large as R=5 when realistic behavior of the structural elements is considered.

The first of the causes mentioned above can be explained by the fact that shorter period structures experience larger seismic demand for the fundamental period ranges mentioned above. The fact that the pseudo acceleration coordinates are larger for T_1=1.80s versus the ones for T_1=2.15s is apparent from **Figure 1**. The second cause of mismatch can be attribute to the fact that the pseudo acceleration coordinates in the reduced spectrum used for the design of the structure is five times smaller than the elastic response spectrum (which matches in a good way the median response spectrum of the realistic case scenario of seismic demand). The latter allows to think that the yielding strength in the realistic behavior of the structure is larger than the one assumed by the codes. This can be explained to occur in the particular building of this research because of the excess of capacity that the columns had for the reason that their flexural design was controlled by minimum requirements.

5.4.2 Realistic Seismic Demand versus Nominal Strengths

The nominal shear strength of the beams and column in the building is dictated by the minimum requirements of transverse reinforcement proposed for intermediate moment framed structures by Chapter 21.12 of the ACI 318-05 code. The nominal flexural strength of the beams is governed by the demand

imposed by the reduced design spectrum of the code. The flexural nominal strength of the columns is governed by minimum requirements in almost all the columns at every level except for the sections at the first story of Columns 2 and 3; their design is governed by low levels of demand that required small quantities of longitudinal steel (ρ<1.70%).

The nominal shear strength of the wall is governed by the elastic demand in the first story and by minimum requirements that satisfy the recommendations of the ACI 318-05 with respect to ordinary reinforced concrete walls. The axial-flexural nominal strength is governed by the demand imposed by the reduced response spectrum from the code.

Using the results shown in **Section 5.3.1** a comparison of demand versus capacity of the structural elements is described in the following paragraphs. In the structure analyzed, there are three levels of correlation between capacity and demand of the structural elements:

- In the first level, the columns' strengths for axial-flexure interaction is larger than almost all the cases of the seismic demand and only some sections at the bottom of the first story were demanded to their probable capacities; the shear strength of the columns is almost twice the 95th percentile level of demand and more than three times the median level. Less than 1% of the 104 events, for which the structure was analyzed, demanded the sections of the columns into the nonlinear range (μ>1).

- The second level of demand versus capacity correlation includes the beams of the frames. As usual, the beams were designed to exceed the level of ultimate demand imposed in flexure by the elastic analysis. Their design for bending moment is characterized by medium levels of longitudinal reinforcement as evidenced by the moderate values of steel quantities (ρ<0.90%). As shown in **Appendix A,** the nominal shear strength of the beams is governed by the minimum requirements of transverse reinforcement rather than the recommendations of Chapter 21.12.3 of the ACI 318-05 code (see **Section 5.3.1**). These strict requirements of the transverse reinforcement enable the sections to sustain large ductility demands thanks to the confined properties of the sections' cores. The flexural demand on the beams was concentrate at their ends because of the existence of bending moment demand imposed by the gravity load. The ductility demand was moderate up to values of μ=7; as it can be confirmed in **Appendix C** the ductility capacity of the beams was always beyond the demand.

- The most demanded element in the structure is, as evidenced throughout this paper, the ordinary reinforced concrete shear wall used to control the drift demand in the elastic analysis. The large stiffness of this element is the cause of the higher values of demand observed in the figures presented in previous sections. The latter fact is the reason why the nominal strength of the wall was at the level of the median demand of the realistic seismic hazard level for both flexure and shear. Even though the analysis of the curvature ductility demand on the wall showed results that exceeded the capacity of the sections only for a few events, **Figure 45** contains a dramatic comparison of the nominal shear strength and the seismic demand on the wall. Only for the two top stories, the nominal shear strength is larger than the median demand from the 104 time series. The fact that the mathematical model used treats the moment and shear interaction as uncoupled, explains why the figure

was able to be constructed. Basically, in the model there is not an upper bound limit for the shear demand in the elements. In reality though, the behavior shown in this figure is not acceptable because, almost always, more than 50% of the events demanded the wall to values that exceeded its shear capacity.

5.4.3 Allowable Story Drift

Even though the allowable inter-story drift limit for the category that the building belongs to is 2.5% (according to the ASCE/SEI 7-05), for the purpose of this paper the structure was designed for a maximum inter-story drift ratio of 1% as recommended by the NSR-98 code. From the pushover analyses, it can be seen that the auto restriction imposed was not as conservative as it seems at first sight.

It is shown in **Section 5.3.2** how the ductility demand is abruptly increased for the walls and the columns of the building for values of roof drift as lower than 0.80%. It is shown in the same section how at levels of roof drift of 2.5% the demand in the columns can exceed their nominal moment strength and how the wall is demanded to values of shear forces much larger than its capacity.

In general it can be said that a structure capable of sustaining an inter-story drift ratio demand of 2.5% has to be designed to have ductility capacities that are not adequately advised in the codes guidelines. An example of the latter assertion is the building codes allowance to use ordinary reinforced concrete walls (which are not design to be ductile elements) in structures that are permitted to undergo story drifts as large as 2.5%.

6 CONCLUSIONS AND FUTURE WORK

Even thought the results presented in this paper are limited to the study of one type of structure, some important annotations and recommendations can be presented with respect to the adequacy of provisions given in building codes with regard to the analysis and design of structures located at intermediate seismic hazard level zones.

i. ***Allowable inter-story drifts****:* it is believed that the acceptance criteria given by buildings codes such as the IBC2006 or the ASCE/SEI 7-05 (see Chapter 12.12 Drift and Deformation), with respect to the maximum drift ratio that an structure belonging to Design Category C can sustain, is set to values (i.e. $\triangle \leq 2.50\%$) that might compromise the overall stability of the structure. Like the case of the ordinary reinforced concrete walls, some elements that might be part of an accepted structural system for this Design Category might not be capable of behave adequately under large ductility demands.

ii. ***Code compliant elastic demand versus realistic demand:*** though they are not conclusive, the results obtained throughout this research project demonstrated that the demand imposed by the reduced design response spectrum proposed by the codes is not even at the median level of demand imposed by realistic scenarios of seismicity. The provisions with respect to the calculation of the shear demand with twice the seismic force contained in Chapter 21.12 "Requirements for intermediate moment frames" of the ACI 318-05 did not seemed adequate either.

iii. ***Ordinary Reinforced Concrete Walls:*** the provision of codes like the IBC2006 in Section 1908.1.4 or the ASCE/SEI 7-05 in Section 14.2.2.5 that recommend the use of ordinary reinforced concrete walls for structures assigned to Seismic Design Category C should be reviewed. Tighter requirements of shear strength and/or evaluation of the shear demand on these walls should be provided. It was demonstrated in this paper, that these elements might experience seismic demands that exhaust their nominal strength capacity. Provisions for Intermediate Reinforced Concrete Walls should be provided by Chapter 21 of the ACI 318 code as they are provided (an proved adequate in this research project) for Intermediate Moment Frames.

In the future, other structural configurations for Intermediate Seismic Design Category are going to be analyzed under the same guidelines used in this paper. The idea is to obtain more general results to be able to draw broader conclusions with regard to the provisions proposed in the building codes with respect to the analysis and design of these structures. Three dimensional models should be used to asses more realistic behavior of the structure; the inclusion of torsional interaction and multidirectional seismic demand will give results that have not been considered in this paper.

REFERENCES

1. *Building Code Requirements for Structural Concrete (318-05) and Commentary (318R-05).* Farmington Hills, MI : American Concrete Institute, 2005.

2. *International Building Code.* s.l., U.S.A. : International Code Council, Inc., 2006.

3. *Minimum Design Loads for Buildings and Other Structures.* s.l. : American Society of Civil Engineers, 2005.

4. *Normas Colombianas de Diseño y Construccion Sismo Resistente.* Santafe de Bogota D.C., Colombia : Asociacion Colombiana de Ingenieria Sismica, 1999. Vol. I.

5. **Watson-Lamprey, Jennie Anne.** *Selection and Scaling of Ground Motion Time Series.* University of California, Berkeley, Ph.D. Thesis, Dept. of Civil and Environmental Engineering. 2007.

6. **Mazzoni, Silvia, et al.** User Command-Language Manual (OpenSees Version 1.7.3). *Open System for Earthquake Engineering Simulation.* [Online] Pacific Earthquake Engineering Research Center; University of California, Berkeley, September 2006. http://opensees.berkeley.edu/OpenSees/manuals/usermanual/index.html.

7. **Yang, Tony and Schellenberg, Andreas.** OpenSees Navigator. [Online] http://peer.berkeley.edu/OpenSeesNavigator/index.htm.

8. *Spectral shape, epsilon and record selection.* **Baker, Jack W. and Cornell, C. Allin.** 9, s.l. : John Wiley & Sons, Ltd., July 25, 2006, Earthquake Engineering and Structural Dynamics, Vol. 35, pp. 1077-1095.

9. **Bozorgnia, Yousef and Bertero, Vitelmo V.** *Earthquake Engineering.* s.l. : CRC Press LLC, 2004.

10. **Bray, J. D.** CE 275 Class Notes. *Geotechnical Earthquake Engineering.* s.l. : University of California Berkeley, Fall 2006.

11. **Chopra, Anil K.** *Dynamics of Structures.* 2nd. Upper Saddle River : Prentice Hall, 2001.

12. **Filippou, Filip C.** CE 220 Class Notes. *Structural Analysis, Theory and Applications.* s.l. : University of California Berkeley, Fall 2005.

13. **Filippou, Filip C.** CE 221 Class Notes. *Nonlinear Structural Analysis.* s.l. : University of California Berkeley, Spring 2006.

14. **Lay, Thorne and Wallace, Terry C.** *Modern Global Seismology.* San Diego : Academic Press, 1995.

15. **Mahin, Stephen A.** CE 227 Class Notes. *Earthquake Resistant Design.* s.l. : University of California Berkeley, Spring 2006.

16. **Mazzoni, Silvia, McKenna, Frank and Fenves, Gregory L.** Example Manual (OpenSees Version 1.7.3). *Open System for Earthquake Engineering Simulation.* [Online] Pacific Earthquake Engineering Research Center; University of California, Berkeley, December 2006. http://opensees.berkeley.edu/OpenSees/manuals/ExamplesManual/HTML/.

17. **Moehle, Jack P.** CE 244 Class Notes. *Reinforced Concrete Structures.* s.l. : University of California Berkeley, Fall 2005.

18. *Ductility of Square-Confined Concrete Columns.* **Park, Robert, Priestley, M. J. Nigel and Gill, Wayne D.** ST4, April 1982, Journal of the Structural Division, ASCE, Vol. 108, pp. 929-951.

19. **Somerville, Paul.** Sources of Conservatism in Current Time History Matching Practice. *Los Angeles Convention Center Hotel Project Review.* December 19, 2006. Los Angeles Convention Center Hotel Project Review.